A Suction-Based Reversible Attachment and Locomotion Mechanism for an Underway Vessel Hull Cleaning and Inspection Robot

by

Alban Cobi

Submitted to the Department of Mechanical Engineering
in partial fulfillment of the requirements for the degree of

Master of Science in Mechanical Engineering

at the

MASSACHUSETTS INSTITUTE OF TECHNOLOGY

May 2020

Author .....
Department of Mechanical Engineering
May 15, 2020

Certified by .....
Douglas P. Hart
Professor
Thesis Supervisor

Accepted by .....
Nicolas Hadjiconstantinou
Chairman, Department Committee on Graduate Theses

A Suction-Based Reversible Attachment and Locomotion Mechanism for an Underway Vessel Hull Cleaning and Inspection Robot

by

Alban Cobi

Submitted to the Department of Mechanical Engineering
on May 15, 2020, in partial fulfillment of the
requirements for the degree of
Master of Science in Mechanical Engineering

Abstract

The international merchant vessel fleet is in charge of carrying over 90% of the items that are traded globally. Any vessel down time brings significant additional costs to the industry. A common source of vessel downtime is the colonization of the vessel hull by marine life, known as permanent marine bio growth. Marine bio growth brings significant risks and costs associated with it, the most notable being a hull frictional drag increase, which significantly increases the annual fuel and maintenance costs of these vessels.

To mitigate these risks and costs, merchant vessels such as cargo tankers undergo a thorough cleaning in a dry-dock up to twice every five years. While saving money in fuel costs and mitigating risks such as the introduction of invasive species, dry-docking can cost over $2,500,000 in a five-year period. Research has shown that adopting a more frequent cleaning regimen, eliminates permanent bio growth and saves maintenance costs, in addition to saving costs associated with the other risks.

A relatively new cleaning regimen has been made possible by in-port cleaning technologies, such as FleetCleaner and HullWiper that make use of manual and semi-autonomous tethered robots with high power vacuum systems that clean and inspect vessel hulls while they are docked for cargo loading and unloading. These technologies are in their infancy so there are no published studies about the costs associated with this in-port cleaning regimen.

There are however some downsides to these technologies that have not made them adaptable by all countries due to stringent regulations against cleaning vessel hulls in harbors. Research has shown that the high power vacuum systems used for collecting the cleaned bio growth do not fully eliminate the risk of the leaching of invasive species and toxic hull coatings into the harbor. Additionally, research shows that magnetic attachment systems, employed by many of these technologies can damage the ship hull coatings which can leach the toxic coatings into the harbor and add additional costs for re-coating the vessel hull.

Studies have shown that a new cleaning regimen, that cleans the vessel hull continuously can dramatically reduce risks associated with bio growth. This cleaning regimen could only be made possible by underway vessel hull cleaning (UVHC) with autonomous robots. There are currently no products that can perform UVHC, however in 2009 Raytheon Company patented a new cleaning and inspection concept of a robot that can perform UVHC. Their concept is attractive in theory but there have not been published feasibility analyses and the robot has yet to be realized.

This work assesses the feasibility of using suction-based attachment for UVHC with compliant bio-inspired suction cups, due their reported resistance to high detachment forces. We introduce a model for studying close-proximity suction-based attachment using a compliant suction cup, and experimentally derive scaling relationships for the detachment force, detachment time, and lateral forces on a suction cup. Using these scaling relationships and a thorough literature review of current attachment and locomotion mechanisms, a new low-power, reversible attachment and locomotion mechanism is presented for the UVHC application.

A proof-of-concept prototype of the mechanism is designed, fabricated and tested in-air and the details of the design are presented in this thesis. The technology shows promise that it can be used as an attachment and locomotion system in energy and power-constrained environments. By supplementing the system with an active attachment system, it may increase the reliability of the device. The mechanism may be useful in other fields such as for inspection and cleaning of underwater structures such as nuclear plants, underwater pipelines, and docked boats.

Thesis Supervisor: Douglas P. Hart
Title: Professor

Acknowledgments

I would like to thank my advisor, Doug Hart for giving me the opportunity to work with him during the last three years. He has truly taught me how to be an independent researcher. He has supported all my endeavors in graduate school thus far, including spending a summer interning in Russia at Skoltech and encouraging me to take classes at MIT that I would've never taken under another advisor. Classes that arguably had nothing to do with my research topic, such as probability and statistics (6.041/6.431) and controls (2.14/2.140), the two most math heavy classes I've taken at MIT apart from classes in the math department. Doug always said math classes are good for you, and now I see why. So thank you Doug.

To my friends and colleagues who have helped and supported me during my time at MIT, I say thank you. I couldn't have done this without your support and help.

To my UROPs, Wendy Bae, Harith Morgan, Sabrina Hare, Amro Alshareef, Mujtaba 'Muji' Jebran, Muhammad Haider, and last but certainly not least Yashasvi 'Yashas' Raj. Thank you for all your help and dedication to this work.

To my Edgerton Center family, thank you for always being there for me and willing to help me with anything I need, even if it's a free cup of iced coffee.

To my family, thanks for supporting me with this "grad school endeavor" that I took on after being out of school for over 5 years. It was difficult, but I couldn't have done it without you.

And to my lovely wife, thank you for putting up with me during the last three years, especially during my quals. Thank you for everything. I love you my zaychik. :)

Contents

List of Figures

List of Tables

Chapter 1

Introduction

Marine vessels including oil tankers, commercial container ships, bulk carriers, and cruise liners are essential in the transport of oil, goods and people. Despite being the oldest and slowest form of transportation, marine transport remains the most fuel efficient on a per tonne of cargo-mile traveled basis, than cars, trains, and airplanes [43]. In 2017, the world's commercial shipping fleet was responsible for transporting over 11×10^9 tons of goods across the globe [48] and in 2018, the market value of water transportation was nearly $550 billion USD [4]. These figures are only projected to grow due to growing populations and an increasingly global economy [4, 48]. It is no surprise then that in the twenty first century as much as 90% of the global trade is carried by the international water transportation industry [21].

This reliance on marine transport means the world's shipping fleet is imperative to the global economy and it means that any costs associated with ship downtime or failure are considered significant losses to the industry. One common reason for vessel downtime is due to the vessel surfaces fouling with organic growth [39]. Marine bio growth, as shown in Fig. 1-1 occurs naturally on submerged surfaces such as vessel hulls, as surfaces in underwater environments present ideal settings for bio growth to occur [6, 33, 26].

Marine life begins to colonize a surface within hours to a few weeks of being submerged in nutrient rich water [6]. Initially, the growth attaches reversibly but after this initial attachment, marine organisms secrete an extracellular polymeric substance

Figure 1-1: Example of marine bio growth on a boat [28].

(EPS), which forms an irreversible bond to a surface. Figure 1-2 on page 16 shows a cartoon of the five temporal stages of bio growth attachment on a surface [6]. The rate and types of growth vary based on the environment, but generally heavy permanent growth from algae, barnacles and mussles such as in Fig. 1-1 occurs on surfaces that have been left underwater on the order of months to years [26, 6].

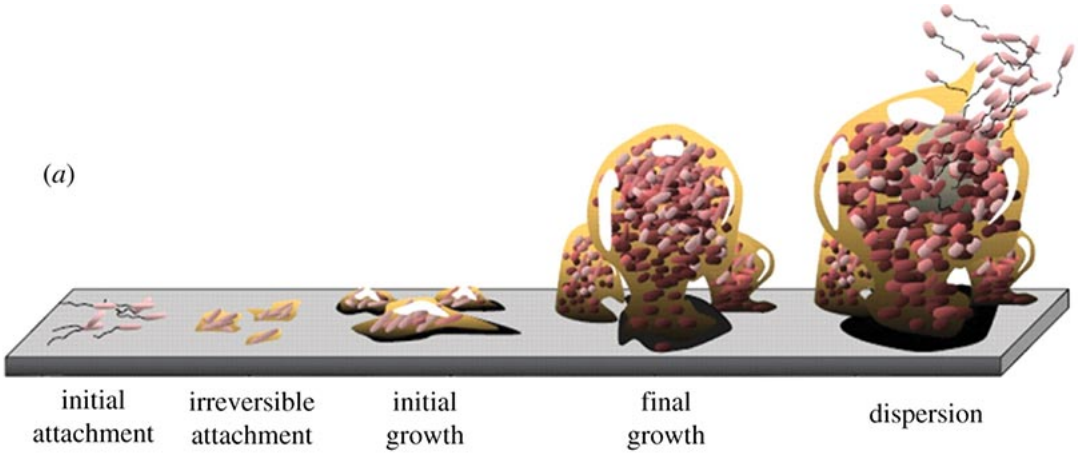

Figure 1-2: Cartoon depicting the five temporal stages of bio growth colonization (adapted from G. Bixler).

1.1 Marine Bio Growth on Vessel Hulls: Problems, Prevention, & Cleaning

Bio growth can occur on any surface of a vessel that is exposed to water. Figure 1-3 below, shows the various parts of a vessel that are susceptible to bio growth, of which the vessel hull (not highlighted) makes up the largest area.

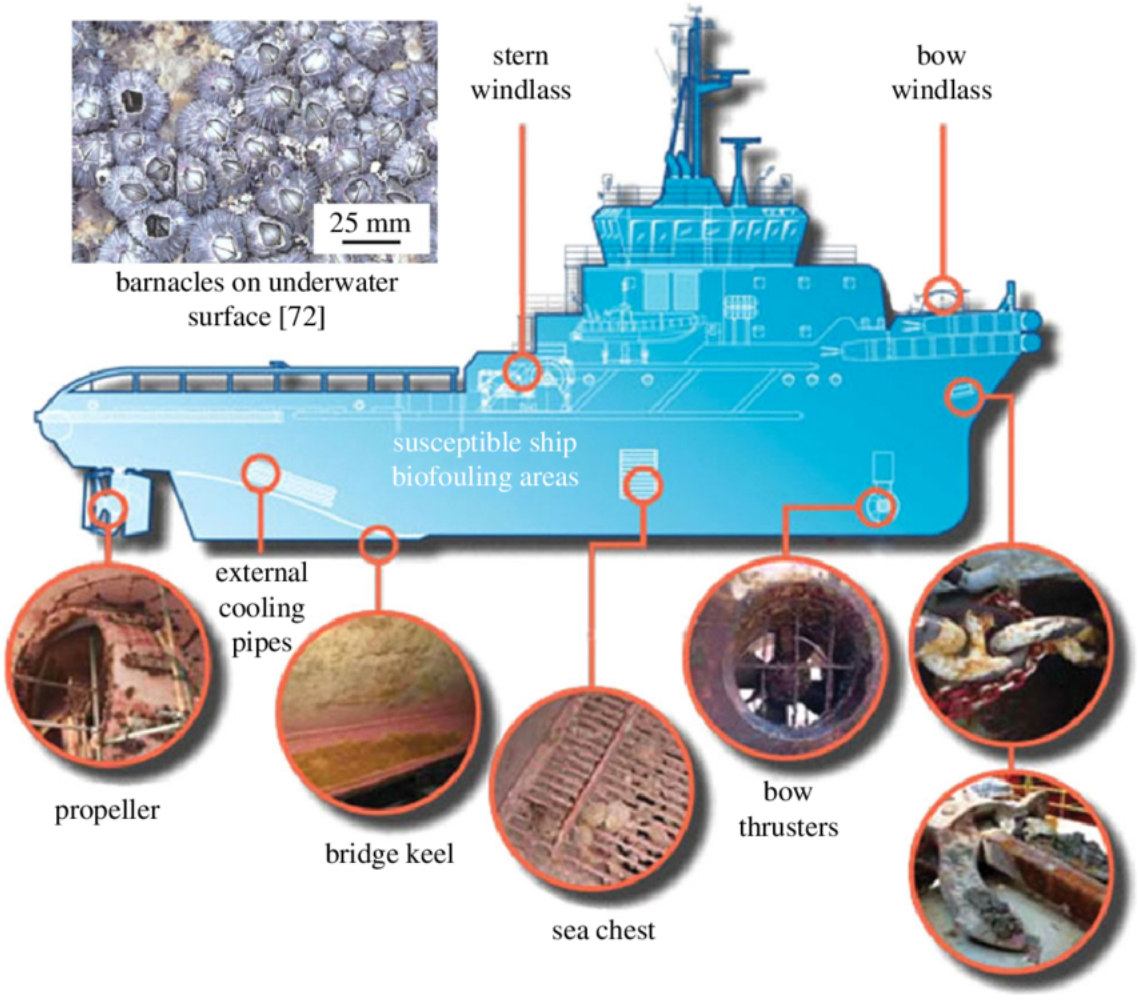

Figure 1-3: Schematic highlighting parts of a vessel that can experience bio growth (adapted from G. Bixler).

The main types of risks associated with bio growth on vessel hulls are health, environmental and financial [40, 39, 6]. Specifically, bio growth on the hull causes the immediate problem of increased frictional drag force on the vessel, which in turn increases fuel consumption and costs associated with travel [39]. This and other well-

known indirect problems and the risks associated with marine bio growth on vessel hulls are outlined in Table 1.1.

Problems	**Risks**
Increased drag force, increases fuel consumption and operational costs, decreases speed of vessel	Environmental, Financial
Introduction of invasive species poses environmental hazards and increases costs of cleaning	Environmental, Financial
Slippery surfaces pose health risks to ship operators and increase medical costs	Health, Financial
Microbially-induced corrosion increases vessel maintenance costs, poses dangers to life in coastal waters due to leaching of toxic paints/coatings in harbors, and health hazards up the food chain	Environmental, Health, Financial
Required regular cleaning and re-coating of fouled areas increases maintenance costs	Financial

Table 1.1: Problems and types of risks associated with marine bio growth on vessel hulls.

To mitigate these risks, the main hull bio growth prevention methods consist of anti-fouling (AF) coatings and copper-based paints, but they do not fully prevent bio growth. After an initial layer of bio film permanently anchors onto the coated hull, larger growth, such as mussels and barnacles begin to populate the surface. There is active research into AF coatings and surface treatments to reduce or eliminate the onset of growth but they have either not succeeded in fully preventing bio growth, have been shown to be toxic or are too expensive to implement on a large scale [38, 39]. Due to the lack of prevention technologies, the main method of effectively removing bio growth is to clean it after it has already permanently attached.

This thesis mainly focuses on the cleaning of bio growth from merchant vessels such as container ships, oil tankers, bulk carriers and cruise liners due to their large hull area, fuel consumption, and the global area covered throughout their lifetime on the water. Due to their large size and state regulations it is costly and non-trivial to clean final stage bio growth from these types of vessels [39, 3, 9].

Traditionally, the cleaning regimen for these large-sized vessels consisted of dry-docking them, then cleaning and painting them using specialized robots or manually by workers on scaffolding [1, 39, 6, 11]. For example, a modern-day Panamax tanker gets dry-docked and cleaned twice every five years, costing upwards of $2,500,000 per five-year period in drydocking costs alone [3]. Due to these high associated drydocking costs, marine vessels of this size have their hulls inevitably become populated by permanent bio growth, which leads to the problems stated in Table 1.1.

A more frequent cleaning regimen has been made possible by recent advances in in-port cleaning technologies. These in-port cleaning systems usually consist of a human-controlled or semi-autonomous cleaning robot that is deployed while the ship is getting loaded and unloaded. These robots clean the hull and contain the fouling from leaching into the harbor using high power vacuum pumps. Due to stringent regulations however, not every country allows in-port cleaning because of the persistent risk of leaching invasive species, toxic paints and AF coatings into the harbor during the cleaning process [9, 49].

Research suggests that increasing the frequency of the hull cleaning reduces the onset of large permanent bio growth and significantly decreases the frictional drag force and related costs [33, 39]. For example, experimental results have shown that increasing the frequency of the hull cleaning for a US Naval ship hull to every 3 to 24 days, only allows a light biofilm to form on the AF-painted surface [47, 39]. A cost study in 2011 by Schultz et. al. suggests that increasing the frequency of cleaning to significantly to reduce maintenance costs is feasible if the vessel is proactively cleaned by multiple autonomous robots. Schultz' results sound promising, however an autonomous robot or service able to continuously clean a vessel hull is yet to be realized. We hypothesize that this is due to the fact that ship hull grooming may require an entirely new system design.

1.1.1 State-of-the-Art in Vessel Hull Cleaning & Inspection Robots

Current state-of-the-art cleaning robots perform the dual-purpose of cleaning and inspecting vessel hulls due to the dire need to inspect hulls for cracks, mines and other issues. In-port cleaning robots such as FleetCleaner (FleetCleaner, Netherlands) and HullWiper (HullWiper, Norway), shown in Fig. 1-4 are currently used in some ports around the world to clean and inspect marine vessels while docked. For reference [11] has a non-exhaustive compiled list of cleaning and inspection robots and specific technical information that was available for each device, as of 2016.

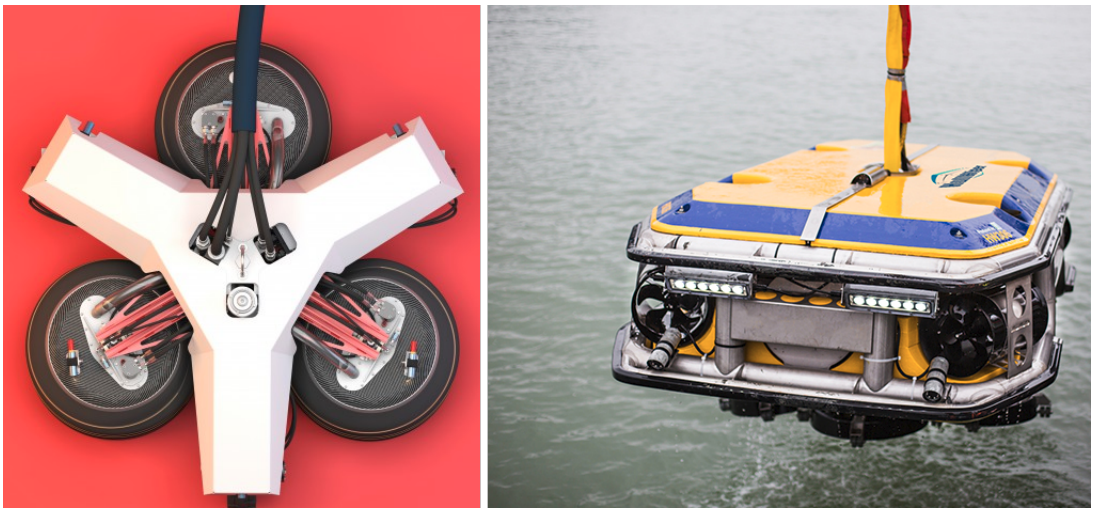

Figure 1-4: (left) FleetCleaner robot and (right) HullWiper robot.

Most of these devices use high pressure water jets or brushes to clean the hull and permanent magnets or thrusters to stay attached to the hull. For example, HullWiper uses thrusters and waterjets to clean the hull surface and requires a nearly 50 kW power supply to clean and traverse the hull surface [19]. FleetCleaner claims to have cleaned over 300 hulls since its inception and HullWiper performed it's first hull cleaning in April of this year (2020) [17, 20]. Costs associated with in-port cleaning were unable to be found online or in scholarly papers. We hypothesize that companies do not have accurate cost estimates or do not generally share the costs due to the infancy of the technology.

1.2 Underway Vessel Hull Cleaning (UVHC) Concept

As mentioned in 1.1, increasing the frequency of hull cleaning reduces the onset of permanent bio growth and consequently the costs and risks associated with permanent bio growth (Table 1.1). A novel solution to cleaning and preventing the onset of permanent bio growth is to continuously clean the hull while the vessel is underway using a tetherless autonomous robot that leeches energy off of the moving flow around the hull. In 2009, Raytheon Company (Waltham,MA,USA) filed numerous US patents on a "hull robot with rotatable turret" and its steering, drive, and navigations sytems for use in UVHC [36]. For simplicity, we will use the term "hull crawler" to describe the autonomous robot used in this manner, for this application, for the remainder of this thesis. Figure 1-5 shows a conceptual model of Raytheon's hull crawler.

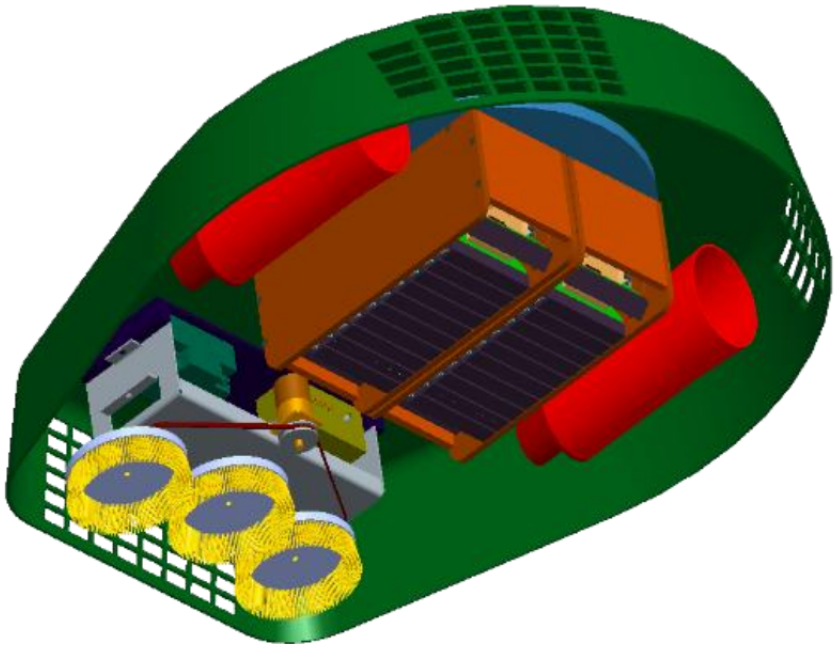

Figure 1-5: Concept of Raytheon's hull crawler, for cleaning ship hulls while underway (adapted from A. Curran [11]).

The main direct advantage of a hull crawler over existing systems is that it operates autonomously and tetherlessly, eliminating the need for human resources while the ship is underway. Using this hull cleaning concept, a cleaning scheme for the target

vessel could look like this:

1. Vessel is dry-docked and cleaned and painted.

2. When vessel is redeployed in the water, numerous hull crawlers are deployed and attached to the vessel hull.

3. When vessel departs, as soon as it is a legal distance from the shore to begin cleaning, the hull crawlers begin to continuously clean the hull.

4. When the vessel arrives near its destination the hull crawlers stop cleaning to comply with local regulations.

5. While docked, the hull crawlers are detached from the hull and cleaned in a freshwater bath, and inspected for damage/replacement.

There are numerous advantages to this cleaning scheme. First, the risk of the introduction of invasive species is reduced due to continuous cleaning. Second, the non-aggressive cleaning methods would reduce the leaching of toxic paints and AF coatings into the water. Third, this would reduce overall maintenance costs associated with dry-docking and may completely eliminate the need for in-port cleaning. Fourth, the vessel would travel faster with increased fuel economy due to less frictional drag. Lastly, this cleaning regimen would comply with international cleaning regulations because a specific country's regulations do not hold in international waters.

1.2.1 Concept Feasibility Analysis

There is limited to no information in literature regarding the feasibility of a hull crawler for the UVHC concept due to the fact that a UVHC hull crawler has never been realized. Furthermore, with a lack of existing products, in order to more accurately assess the feasibility we must evaluate the hull crawler based on existing surface crawling robots that perform a variety of different functions. These functions include, vessel hull inspection, vessel hull paint-stripping, and in-air beverage and chemical

tank inspection. In what follows, a first-order feasibility analysis is conducted in order to assess the attachment forces and power generation needed for a hull crawler to perform it's functions without detaching from the ship hull.

First, it is worth noting that the hull crawler, will spend time in three regions of a vessel hull with different dynamics, the air region, air-water region, and underwater region. Figure 1-6 shows a cartoon of these three regions of a vessel hull. For the following analyses it is assumed that a hull crawler spends most of its time in the underwater region, III. In regions I and II, minimal time is spent, but further analysis, out of the scope of this thesis is required to assess the dynamics of the hull crawler in those regions.

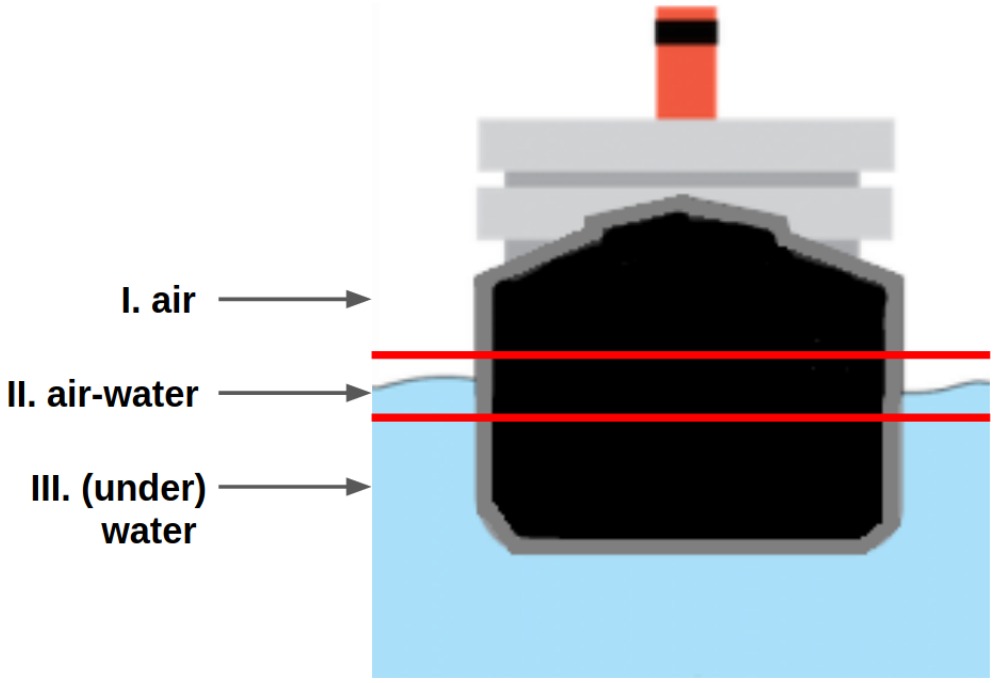

Figure 1-6: Cartoon showing the three regions of a vessel hull.

Attachment Analysis:

Ross et. al. indicated that in the early twenty-first century, only about 100 vessel hull paint-stripping robots were in use worldwide [37]. They cite the lack of market adoption of these robots, primarily due to their unreliable attachment mechanisms, causing robots to fall numerous times during operation [37]. Compared to vessel

hull paint-stripping which is performed on a static vessel in a dry-dock, the UVHC concept requires the robot to attach to a moving vessel in highly dynamic conditions. Therefore, the main force the hull crawler has to withstand is the drag force due to the flow around the hull. A first order analysis to estimate this drag force on a hull crawler attached to a typical merchant ship such as an oil tanker shows that it is on the order of 20 kN, assuming a drag coefficient of unity. For reference, Appendix A shows the details of this calculation.

A first order calculation shows that 12 mm thick neodymium magnets on a bare steel sheet, with a coefficient of static friction of 0.1, encompassing an area of 1 m^2 can withstand this drag force [23, 25]. In reality, an attachment mechanism must able to attach to a ship hull surface which has a mean roughness on the order of 150 microns [39], a non-ferrous paint layer on the order of 700 microns thick [32] and regular asperities such as weld joints, flanges, or marine fouling [37]. This analysis however, shows that attachment can be achieved to with a permanent magnet attachment system.

Power Generation Analysis:

If the hull crawler is to continuously stay attached, move, and clean a vessel hull, without a tether, a reliable power generation system is required. While the moving flow around the hull crawler causes large drag forces, it is also a large source of energy. If this energy could be harnessed to power the hull crawler, without significantly increasing the total drag on the vessel hull, the hull crawler would have a continuous source of power during its operation. This was first proposed by Raytheon in their patent [36]. According to the patent, the robot's primary power needs are due to the drive system, cleaning system, sensors, controls, and a system to rotate a turbine towards the incoming flow to generate power. The attachment system did not require power because it utilized permanent magnets.

As mentioned earlier, by using the UVHC scheme, permanent bio growth is not allowed to form, and therefore the cleaning system would require relatively less amounts of energy to remove a thin layer of bio-film present on the hull surface. Experiments

have shown that it only takes about 50-100 Watts of power to clean a thin bio-film layer off of a painted ship hull with a rotating brush [25].

To validate whether a turbine could provide enough power for Raytheon's hull cleaning crawler concept, a proof-of-concept prototype of a tracked-robot with permanent magnets and a rotating brush cleaning system was demonstrated by students in 2.013, an MIT senior capstone course [25]. The concept showed that a commercially available 600 Watt hydrogenerator (Watt & Sea, France) can provide sufficient power for the application [25]. For reference, Appendix B shows the details of the hydrogenerator.

To conclude, this analysis shows the feasibility of the two critical subsystems of the hull crawler concept, the attachment and power generation. The main focus of this thesis is on the attachment subsystem.

1.3 Analyzing Current Reversible Attachment Methods

Research into different attachment methods shows that there are at least eight mechanisms that are known to cause attachment or adhesive forces between two surfaces, shown in Fig. 1-7. A ninth mechanism, caused by thrust forces directed toward two objects is not shown in Fig. 1-7.

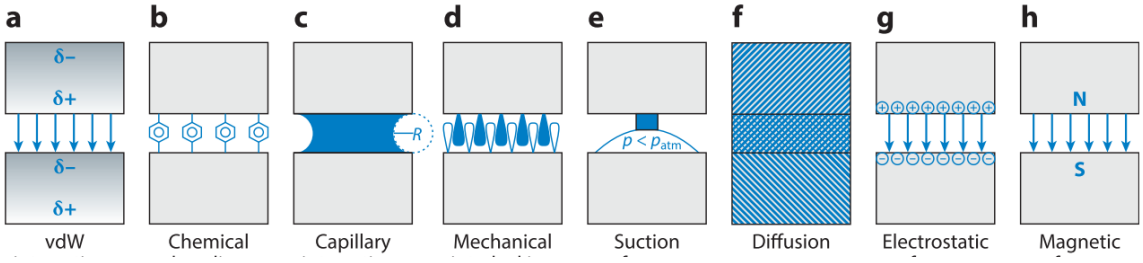

Figure 1-7: Different attachment mechanisms between solid surfaces (adapted from S. Gorb).

Due to their rapid attachment and detachment reversibility, the only mechanisms that are viable for UVHC are capillary action, mechanical interlocking, suction forces,

electrostatic forces, magnetic forces, and thrust forces. Van der Waals and electrostatic forces do not work in the presence of a water film between two surfaces [12]. Capillary forces provide high force per unit area at micrometer length scales so they do not make for viable attachment mechanism on a hull crawler. Therefore, the only viable attachment mechanisms for this application area mechanical interlocking, suction forces, magnetic forces, and thrust forces.

Market research into hull cleaning and inspection robots shows that the current attachment mechanisms implemented on these robots fall into three categories: permanent magnets , thrusters, or negative pressure (suction). For reference, see [11] for a list of hull cleaning and inspection robots and the available details of each robot. Using information from [11] and other current hull cleaning and inspection robots, a pugh chart was created, highlighting important qualities of these attachment systems. The pugh chart, shown in Table 1.2, aims to compare each attachment technology, with regards to implementation on a hull crawler for UVHC.

For ferrous hulls, permanent magnets appear to be the most fitting solution for attachment, due to the zero energy cost of attachment. However, magnetic attachment systems on hull crawling robots for other applications have shown that they have severe limitations. For example, in their analysis of hull paint-stripping robots, Ross et. al. state that it has been reported that magnetically tracked robots such as a crawler by JetEdge (JetEdge, USA) marked the underlying paint layers on a vessel hull, during turning and heading correction [37]. Furthermore, they state that magnetically tracked systems are unable to handle curved areas and asperities on the hull surface due to the rigidity of the magnetic system, which deemed them unreliable and prone to falling off of the ship hull. Even if permanent magnet systems can be designed for this application, they would exclude numerous ships that have non-ferrous hulls. Due to these known reasons, magnets were excluded as a viable attachment technology for the UVHC application.

For non-ferrous hulls, mechanical interlocking and suction forces are the only viable attachment mechanisms, as thrusters require large amounts of power to keep an object attached to a vessel hull continuously. We hypothesize that because an un-

	Neodymium Magnets (12 mm thick)	**Thrusters**	**Negative Pressure (Suction)**
Holding Pressure at Hull Surface [Pa]	200 kPa [23]	>100 kPa depending on thruster size	<100 kPa (theoretical maximum at sea level)
Energy Cost of Attachment [Pa/J]	0	very high	high
Friction Coefficient [-]	0.1-0.3 [25]	-	-
Attach to Non-ferrous Surfaces?	no	yes	yes
Reliable on Irregular Surfaces?	no	yes	yes
Damage hull surface?	yes	no	no

Table 1.2: Comparison of different attachment systems on current hull cleaning and inspection robots.

fouled hull is relatively smooth [39], mechanical interlocking would not be effective and may result in stripping paint off of the hull surface. This analysis leaves negative pressure, also known as suction as the only other solution for the attachment mechanism.

1.3.1 Feasibility of a Suction-Based Attachment Mechanism for UVHC

Suction can theoretically attach with a pressure of 100 kPa at sea level which makes its attachment force comparable to 12 mm thick neodymium magnets. Additionally, suction could work on ferrous and non-ferrous surfaces but may only be viable if it is able to resist the detachment forces present in the application, primarily due the drag

force calculated in 1.2.1. Current suction-based systems such as the Vectored Little Benthic Crawler (vLBC), a hull inspection robot by SeaBotix, uses active suction technology to attach to hull surfaces with a total force of over 210 Newtons. This force divided by the area footprint of this robot results in an attachment pressure just under 900 Pa. Assuming a coulomb friction model, this robot would require a coefficient of friction multiple orders of magnitude greater than unity in order to withstand 20 kN of drag force, which is unrealistic. There is a myriad of research however that shows that suction-based attachment using compliant suction-based grippers can resist normal detachment pressures up to 70 kPa and frictional pressures up to 5 kPa [13, 50, 24, 18].

Compliant suction-based grippers such as [13, 50, 24, 18] can resist higher detachment forces due to the close proximity, $O(\mu m - mm)$ of the gripper to the substrate. Therefore, compliant active grippers such as simple commercially available suction cups require significantly less power to generate attachment forces compared to systems such as that of the vLBC, which operate at $O(mm - cm)$ proximity to surfaces. Furthermore, close-proximity suction with elastomeric materials in contact with a ship hull would reduce the risks of damaging the ship hull and could have friction coefficients that are significantly higher than those of permanent magnet systems [35, 29].

First order calculations using the commercially available DURAFLEX FCF125P friction suction cups (PIAB, USA), specifically designed for grasping smooth, oily surfaces, show that these suction cups, comprising an area of 3 m^2 can resist the 20 kN drag force calculated in 1.2.1 [31]. This resistance to detachment forces makes compliant elastomeric suction-based grippers attractive for the application of UVHC with a hull crawler and thus becomes the focus of this thesis.

Chapter 2

Close-Proximity Suction Attachment Physics

In order to design a close-proximity suction-based attachment system for the proposed hull crawler concept that is able to resist the drag force presented in Section 1.2.1 it is necessary to understand the fundamental physics of close-proximity suction-based reversible attachment.

First, we abstract the concept of reversible attachment by breaking down the problem of two surfaces coming into contact into three stages of interest, shown in Fig. 2-1. Stage (I) is the attachment stage, in which two surfaces move relative to each other in order to come into contact. Stage (II) is the attached stage, in which the two surfaces are static relative to each other. Stage (III) is the detachment stage, in which the surfaces again move relative to each other and start to separate.

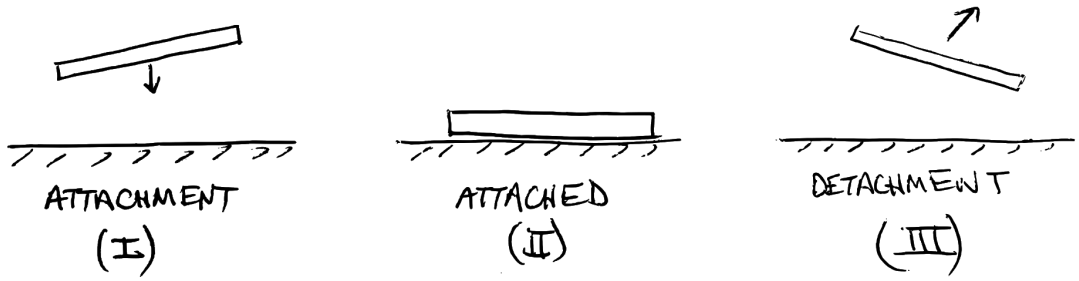

Figure 2-1: A cartoon depicting the three stages of reversible attachment between two surfaces.

In order to design and fabricate a robust attachment mechanism, consideration of these three stages must be taken into account. Due to the complex dynamics that occur at small time scales during the attachment and detachment stages (I and III), most of the analyses herein is focused on the attached stage (II). In stage (II) it is assumed that the two surfaces are static relative to each other. This assumption allows us to model the underlying physics of suction-based attachment under a quasi-steady state assumption.

2.1 Suction Attachment Between Two Solid Surfaces

In order to understand the attachment physics between suction-based grippers such as [13, 50, 24, 18] and substrates, we abstract the problem by using simple geometries as shown in Fig. 2-2.

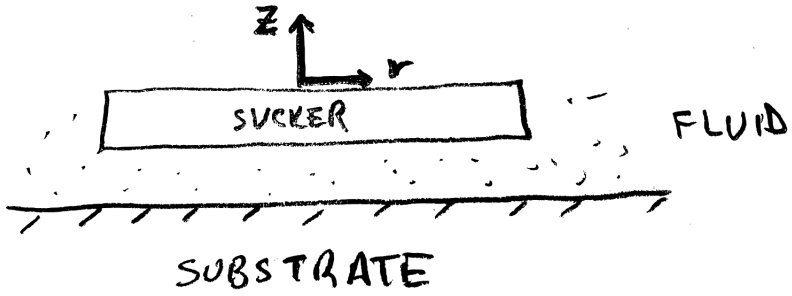

Figure 2-2: A cartoon depicting three basic elements in a suction attachment problem: the sucker, the substrate and the fluid.

Here, we assume the suction gripper or "sucker" for short, is a symmetrical flat disc and the surface it attaches to is called the substrate. The substrate is assumed to be flat and stiff relative to the sucker. This is consistent with the application of merchant vessel hull cleaning because merchant vessel hulls are made of stiff materials such as painted steel, fiberglass, and carbon fiber [7]. In contrast, suction-modules such as [13, 50, 24, 18] are made of elastomeric materials. These assumptions imply that any deformation that occurs, will occur in the sucker. Finally, it is assumed that both sucker and substrate are immersed in a homogeneous fluid.

By definition, suction cannot occur in a vacuum because the pressure field in a vacuum is zero everywhere. Therefore, fluid needs to be present in order for a non-zero pressure field to exist. A low pressure region between two surfaces causes a pressure differential in the fluid field between one side (-z) of the sucker and the other (+z), and this is what creates the "adhesive" effect known as suction.

2.1.1 Active Suction vs. Passive Suction

As mentioned, suction is caused by a region of low pressure between two surfaces. The low pressure region can be caused by either actively doing work to the fluid to move it or by expanding the volume of the region between the two surfaces. We define these two methods as active and passive suction, respectively. The most simple and elegant examples of passive and active suction attachment are demonstrated by what are colloquially known as suction cups. Figure 2-3 on page 31 shows examples of active and passive suction cups in practice.

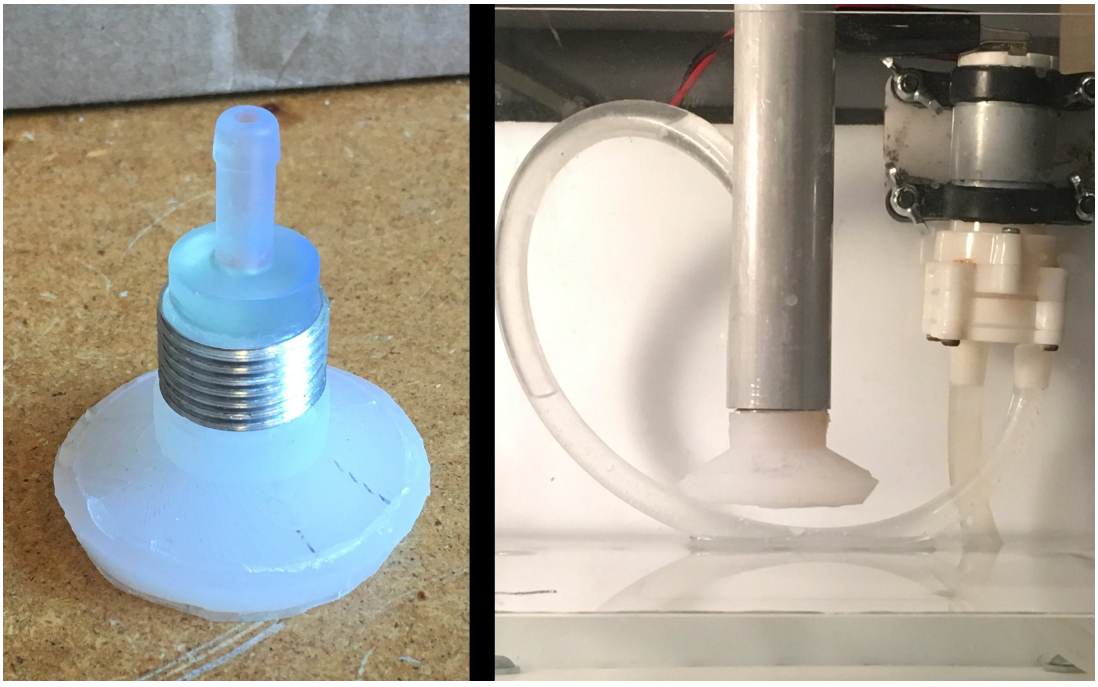

Figure 2-3: Examples of (left) passive vs. (right) active suction.

Active Suction

We define active suction attachment as attachment between two surfaces that is caused by *actively moving fluid* by a mechanical element, such as a pump, in order to create a *time-independent* pressure field in the surrounding fluid domain. Active suction therefore requires a continuous external source of power to drive the mechanical element. The "adhesive effect" is caused by a low pressure region between the two surfaces, due to the motion of fluid. The resulting pressure field integrated around the sucker surface area results in a net force on the sucker toward the substrate.

The main advantage of active suction is that in the attached stage (II) the pressure field and therefore the attachment force between the sucker and the substrate is constant (i.e. not time dependent). The biggest disadvantage however, is that constant input power is required in order to maintain a low pressure region that is independent of time. For the application of UVHC with a hull crawler, passive suction is more attractive than active suction because it requires less input energy to provide attachment.

Passive Suction

We define passive suction attachment as attachment between two surfaces that is caused by the *expansion of the volume between the two surfaces* in order to create a *time-dependent* pressure field in the surrounding fluid domain. We assume the energy to expand the volume is caused by a finite energy storage element. The "adhesive effect" is caused by a low pressure region between the two surfaces, due to the action of a "separation force" acting on either of the two surfaces. This separation causes volume expansion and a local region of low pressure between the two surfaces. This local region of low pressure causes fluid to flow between the two surfaces, and this flow creates a pressure field between the two surfaces that when integrated, causes a net attractive force between them.

The advantage of passive suction is that it uses less energy (i.e. the energy in the finite storage element), however this results in a pressure field, and hence an

attachment force that is time-dependent. After the stored energy is used, suction attachment is lost. Due to the time-dependence, the physics in passive attachment is more complicated. In the following analyses we will make the quasi-steady assumption and apply fluid and contact mechanics, to arrive at scaling solutions and some closed-form analytical solutions for the separation force, detachment time, and lateral force between two surfaces in close-proximity suction.

2.2 Close-Proximity Suction with Small Deformations: Stefan Adhesion

First, we take a look at a classical problem known as Stefan Adhesion in which two rigid surfaces, a disc of radius R, and a substrate, with a newtonian fluid between them experience an "adhesive effect", by the action of an external separation force. The problem geometry is shown in Fig. 2-4. In the following analyses we aim to solve for the separation force, detachment time, and friction force as a function of the geometrical parameters of the disc and fluid material properties.

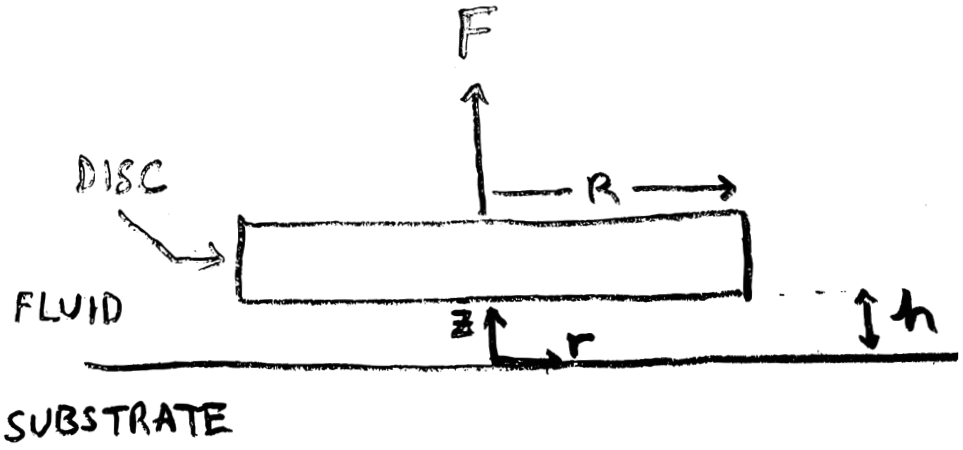

Figure 2-4: Diagram depicting stefan adhesion between a disc and a substrate.

The following assumptions are made in the following analysis:

1. Smooth substrate and disc surface (i.e. surface roughness « h)
2. Elastic deformations in disc/substrate « h
3. Disc and substrate never come into contact
4. Newtonial, incompressible fluid of viscosity μ
5. Axisymmetric flow with Re « 1
6. h « R

By assuming quasi-steady conditions and applying the differential form of continuity and the navier-stokes equations on a differential volume in the fluid domain, in the e_r direction, and applying lubrication theory under assumptions 5 and 6, we can solve for the resulting velocity profile of the fluid, given by Eq. 2.1.

$$v_r(z) = \frac{1}{2\mu}\left(zh - z^2\right)\left(-\frac{dP}{dr}\right) \tag{2.1}$$

Then, we can obtain two expressions for the volumetric flow rate, one from integrating the velocity profile over a cylindrical area at an arbitrary distance, r under the disc, and the other by applying the integral form of continuity on a cylindrical control volume under the disc, resulting in Eq. 2.2 and Eq. 2.3, respectively.

$$Q(r) = \frac{\pi h^3}{6\mu}\left(-\frac{dP}{dr}\right) r \tag{2.2}$$

$$Q(r) = \pi r^2 \frac{dh}{dt} \tag{2.3}$$

Equating these two expressions and solving for the pressure, $P(r)$ results in the following expression for pressure:

$$P(r) = P_{atm} - \frac{3\mu}{h^3}\frac{dh}{dt}\left(R^2 - r^2\right) \tag{2.4}$$

The above result states that the pressure distribution under the rigid-disc is parabollic, as shown in Fig. 2-5.

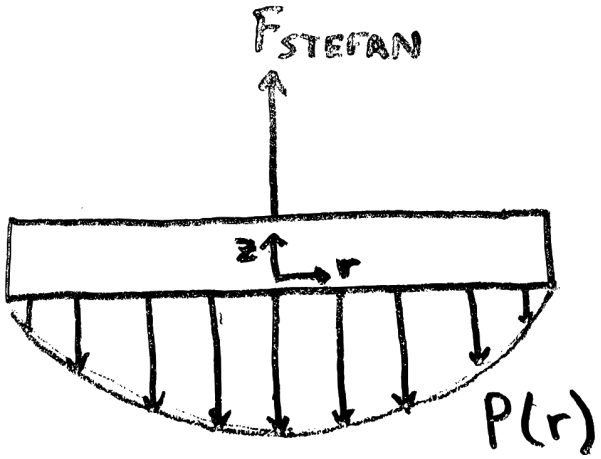

Figure 2-5: Quasi-steady pressure distribution under rigid disc.

Separation Force

Next, by applying a force balance on the disc in the e_z direction, the separation force is derived, shown by Eq. 2.5. The "adhesive effect" that is caused by this separation force is known as stefan adhesion, first derived by Stefan in 1875 [44].

$$F_{stefan} = \frac{3\pi\mu R^4}{2h^3}\frac{dh}{dt} \tag{2.5}$$

Separating out the terms in Eq. 2.5 gives insights into how each variable in the problem contributes to the "adhesive effect":

$$F_{stefan} = \left(\frac{3\pi}{2}\right)(\mu)\left(R^4\right)\left(\frac{1}{h^3}\frac{dh}{dt}\right) \tag{2.6}$$

Equation 2.6, shows that the separation force between the two rigid surfaces is proportional to the fluid viscosity, the radius of the disc, and a more complicated term that captures the gap height, h and separation speed, $\frac{dh}{dt}$ between the two surfaces. In other words, the physics of this suction problem is dominated by a material property, geometric properties, and the separation speed. From the design perspective if we want to solely rely on passive suction for a given attachment force, these are the only variables we have control over.

Detachment Time

Next, in order to calculate the time until the two surfaces detach from each other, assuming a constant separation force, $F_{stefan} = constant$ we can take Eq. 2.5 and solve for $h(t)$ by integrating assuming an initial height h_o. The dimensionless expression for $h(t)$ is given by:

$$\frac{h}{h_o}(t) = \left(1 - \frac{F_{stefan} h_o^2 t}{12\pi\mu R^4}\right)^{-\frac{1}{2}} \tag{2.7}$$

Now we can solve for time of detachment, t_{detach} by assuming that $h(t_{detach}) \to \infty$:

$$t_{detach} = \frac{3\pi\mu R^4}{4h_o^2 F_{stefan}} \tag{2.8}$$

Again, separating out the terms in Eq. 2.8 gives insights into how each variable in the problem contributes to the detachment time:

$$t_{detach} = \left(\frac{3\pi}{4}\right)(\mu)\left(R^4\right)\left(\frac{1}{h_o^2}\right)\left(\frac{1}{F_{stefan}}\right) \tag{2.9}$$

Equation 2.9 is better used to understand the scaling of the the detachment time with the parameters of the problem.

Lateral Force

Next, we now consider a lateral force acting on the disc in addition to the separation force, causing it to move at a constant horizontal velocity, v relative to the substrate. Given assumption 3, the fact that the disc and substrate never come into contact, the horizontal force on the disc is simply the shear force on the fluid multiplied by the area of the disc. Given assumption 4, that this is a newtonian fluid the shear force, τ_{wall} is given by the definition of viscosity:

$$\tau_{wall} = \mu\frac{dv}{dz} = \mu\frac{v}{h} \tag{2.10}$$

Multiplying this result by the disc area yields the following expression for the lateral force, $F_{lateral}$ on the disc:

$$F_{lateral} = \pi \mu R^2 \frac{v}{h} \tag{2.11}$$

Again, as we did before, separating out the terms gives insights into how the lateral force on the disc should scale:

$$F_{lateral} = (\pi)\,(\mu)\left(R^2\right)\left(\frac{1}{h}\right)(v) \tag{2.12}$$

In practice, Equations 2.6, 2.9, and 2.12 for the detachment force, F_{stefan}, detachment time, t_{detach} and lateral force, $F_{lateral}$ are better used as scaling relationships based on the parameters of the suction geometry given by Fig. 2-4. Calculating the exact numbers for a real suction-problem requires an experiment to be conducted. From a design perspective these variables are very limiting. Unfortunately a robot cannot actively control the surface it is going to attach to or the fluid it is going to be submerged in, unless the robot carries a tank of fluid that it can inject in the vicinity of the attachment. Therefore, the only element of attachment a designer has freedom over is the sucker. Compliant suckers such as [13, 50, 24, 18] allow for many more design possibilities, however these can come at a higher cost of complexity, as we later discuss in Chapter 3.

2.3 Close-Proximity Suction with Large Deformations

In order to model compliant suckers made of elastomeric materials such as [13, 50, 24, 18] we choose to first model a basic geometry such as a suction cup. The reason for choosing to model a suction cup is because is it a symmetrical geometry that attaches by passive suction through the energy stored in it by elastic deformations. It does not require large amounts of external energy or the action of an external separation force in order to attach, which makes it ideal for the UVHC application, where energy is limited.

We will model the suction cup as a compliant cone that elastically deforms into

a disc when it comes into contact with a flat rigid substrate. A diagram of this attachment process is shown in Fig. 2-6, where attachment occurs under the action of an external force pushing the cone toward the substrate. Similar to the analyses in Section 2.2, we aim to solve for the separation force, detachment time, and lateral force as a function of the geometrical parameters and material properties of the cone, and the fluid material properties.

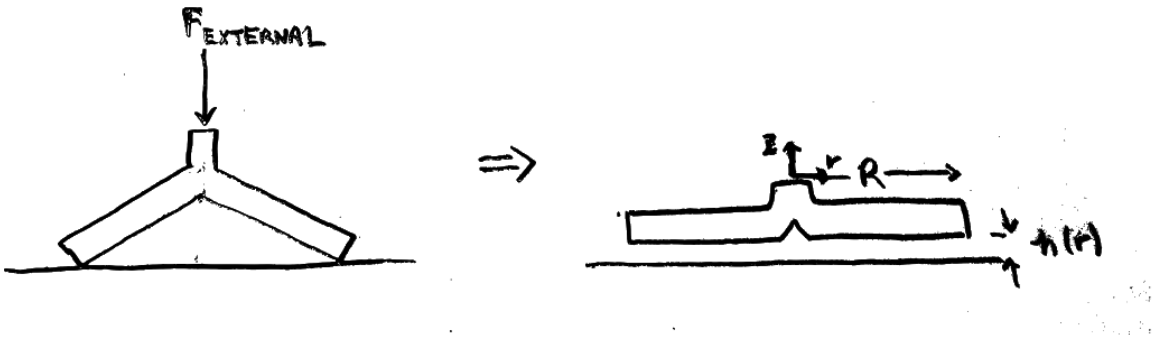

Figure 2-6: Diagram showing attachment of a compliant cone.

The following assumptions are made in the following analysis:

1. Rough substrate (i.e. surface roughness » h)
2. Smooth cone surface (i.e. surface roughness « h)
3. Stiff substrate (i.e. Elastic deformations « h)
4. Compliant cone (i.e. Elastic deformations » h)
5. Cone and substrate come into contact
6. Newtonial, incompressible fluid of viscosity μ
7. Axisymmetric flow with Re « 1
8. h « R

Again, we start the analysis assuming quasi-steady conditions, and apply the navier-stokes equation and continuity on a differential volume in the fluid domain between

the two surfaces to arrive at the same result as Eq. 2.1 for the fluid velocity profile. Integrating this velocity profile over a cylindrical area at an arbitrary distance, r, yields an equivalent expression to Eq. 2.2 for the volumetric flow rate, $Q(r)$ leaking into the cavity. Separating out the terms in Eq. 2.2 yield the following expression:

$$Q(r) = \left(\frac{\pi}{6}\right)\left(\frac{1}{\mu}\right)\left(h(r)^3\right)\left(-\frac{dP}{dr}r\right) \tag{2.13}$$

Next, for simplicity, we assume a step input external separation force is applied to the sucker at time, $t = 0$. Experiments have shown that under a large enough separation force, a vapor bubble begins to form in the cavity [14]. Under these conditions and under the quasi-steady assumption, we assume that the flow rate given by Eq. 2.13 is constant and independent of the radius, r. These assumptions allows us to solve for the quasi-steady pressure distribution under the sucker, by integrating the flow rate over the radius, which results in the following expression for the pressure distribution in the incompressible fluid doman:

$$P(r) = P_{atm} - \frac{6\mu Q}{\pi h(r)^3} ln\left(\frac{r}{R}\right) \tag{2.14}$$

The above result states that the pressure distribution in the incompressible fluid domain under the sucker is logarighmic, with the lower bound being the cavitation pressure of water at the given temperature, as shown in Fig. 2-7. It is important to note that in this analysis we treated h as independent of r but in reality the pressure will drop to atmospheric much faster than a logarithmic relationship because the gap height increases radially outwards, due to the highly deformable sucker. This result however allows us to understand that the pressure distribution under the compliant sucker is highly different from the rigid disc in stefan adhesion. This may result in the scaling relationships for separation force, detachment time, and lateral force to differ from the stefan adhesion results.

Separation Force

Next, following the same analysis as in stefan adhesion, a force balance on the sucker

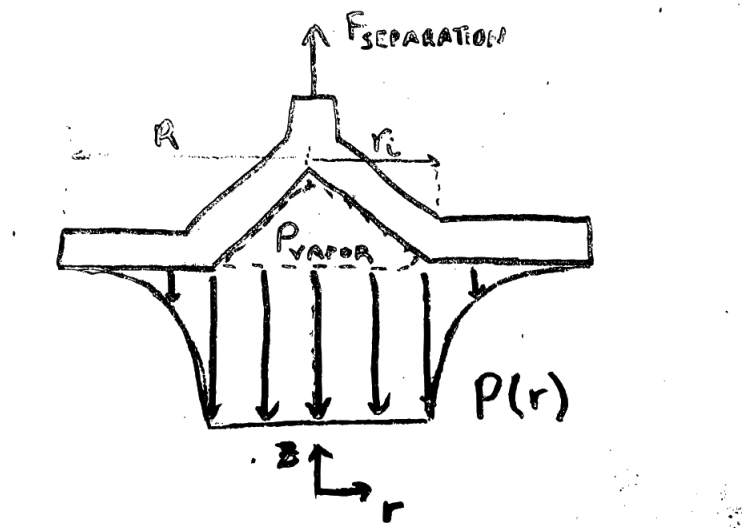

Figure 2-7: Quasi-steady pressure distribution under compliant cone.

in the e_z direction yields Eq. 2.15, also shown graphically in Fig. 2-8.

$$F_{separation} = \Delta P_{vapor} Area_{vapor} + \int_{r_i}^{R} \Delta P(r) dA - N_{total} \tag{2.15}$$

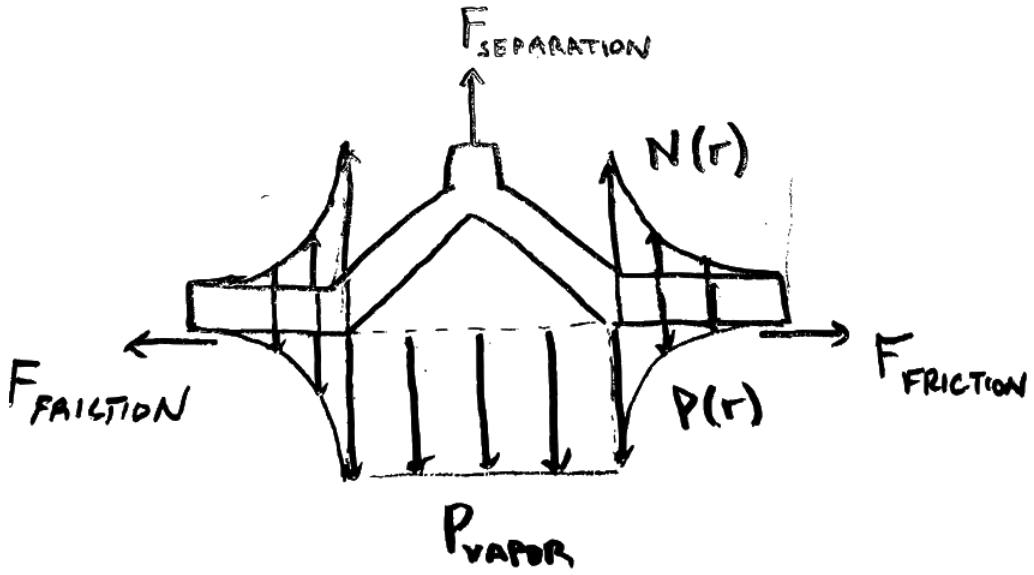

Figure 2-8: Force balance on compliant cone.

Since the suction cup is under compression in the region where it contacts the substrate, this implies the pressure forces balance the normal forces,

$$\int_{r_i}^{R} \Delta P(r) dA = N_{total} \tag{2.16}$$

The separation force therefore simplifies to,

$$F_{separation} = \Delta P_{vapor} Area_{vapor} \tag{2.17}$$

Equation 2.17 states that the external force is purely balanced by the the vapor gauge pressure and area of the cavity. Additionally, due to the fact that we assumed contact between the two surfaces (assumption 5), this implies there is contact friction present. This is a key difference between the stefan adhesion (small deformations) case and large deformations case because in the small deformations case, the two surfaces never come into contact. This means that friction plays an important role in suction attachment with compliant suckers.

The presence of contact friction can be validated experimentally due to the fact that the cone does not immediately slip inwards as it is being separated from the substrate. Ditsche et. al. conclude this in their study of northern clingfish attachment [13], but now we have shown some of the complex physics behind this theory.

In order to attempt to determine an analytical relationship between the separation force and the parameters in the problem, the cauchy momentum equation and contact mechanics theory between elastomers and hard substrates must be applied. This is left for future work. What we can conclude for certain however, from the Stefan Adhesion result (Eq. 2.5) and the pressure distribution under a compliant sucker (Eq. 2.14) is that the separation force should at least be a function of the following parameters:

$$F_{separation} = f(\mu, h, v_{separation}, R, \eta, E) \tag{2.18}$$

Where η and E are friction coefficient and the elastic modulus of the sucker, respectively. Therefore the separation force in close-proximity suction with large deforma-

tions is a function of the fluid viscosity, μ geometrical parameters and elastic modulus of the sucker, gap height, h and separation speed $v_{separation}$. In Section 2.4 we perform experiments to show that this force has a weaker dependence on viscosity and separation speed than the stefan relation (Eq. 2.5).

Detachment Time

Next, we obtain a scaling relationship for the time until the two surfaces detach from each other under two scenarios: with a *constant external force*, and with *no external forces* applied to the sucker.

First we derive a scaling relationship for the detachment time by dividing the volume of the cavity of the un-deformed cone, by the flow rate scaling we derived earlier (Eq.2.13). This gives an accurate scaling is because once the cavity volume is filled with incompressible fluid the pressure differential across the sucker will equalize and thus detachment will occur. To arrive at the scaling relationship we assume $dP \sim \Delta P_{cavity}$, where ΔP_{cavity} is the pressure at the center of the cavity. This gives us the following scaling for the detachment time, where H_{cavity} is the height of the cavity of the un-deformed cone.

$$t_{detach} \sim (\mu)\left(\frac{1}{h^3}\right)\left(\frac{R^2 H_{cavity}}{\Delta P_{cavity}}\right) \tag{2.19}$$

This result states that the detachment time should scale with the viscosity of the fluid, the gap height, the geometry of the sucker and the pressure in the cavity. While the gap height, h is difficult to analytically compute, the pressure of the cavity can be obtained by a scaling relationship. Next, we obtain a scaling for this pressure under two different conditions, relevant to the hull crawler application.

Constant External Force Case:

First we consider the case of a constant external separation force applied to the sucker. This case is relevant in the case where there are dynamic detachment forces acting on a hull crawler, such as the forces from turbulence or drag. Plugging in the expression

for the vapor pressure, ΔP_{vapor} that can be obtained from Eq. 2.15 into ΔP_{cavity}, yields:

$$t_{detach} \sim (\mu)\left(R^4\right)(H_{cavity})\left(\frac{1}{h^3}\right)\left(\frac{1}{F_{ext}}\right) \tag{2.20}$$

This equation looks similar to the equation from the stefan adhesion analysis (Eq. 2.9) except that the cavity height appears in the equation due to the fact that the disc is initially conical. This concludes that the geometry and elastic properties of the sucker and the external separation force are important in determining the detachment time.

No External Force Case:

Now we consider the case of no external forces on the sucker, which is relevant in the case where a ship is stationary, such as when it is docked and the hull crawler remains stationary. Under this condition, the sucker will still maintain suction due to the fact that the pressure in the cavity, ΔP_{cavity} is caused by the stored elastic energy in the sucker. To get a scaling for the cavity pressure we can take a cross-section of the cone and observe that each side of the cone is simple beam with elastic modulus, E, of length, L, bending by an amount δ under a distributed load. Under these assumptions, we can arrive at the result that the pressure in the cavity should scale with the applied load induced on the beam due to an imposed strain on the beam. Then, the cavity pressure, ΔP_{cavity} scaling is given by:

$$\Delta P_{cavity} \sim \frac{F_{beam}}{A_{disc}} \sim \frac{\delta EI}{L^3}R^2 \tag{2.21}$$

Where A_{disc} is the area of the cone when flattened into a disc. Plugging this result into the detachment time scaling (Eq.2.19) yields:

$$t_{detach} \sim (\mu)\left(\frac{1}{h^3}\right)\left(\frac{R^4 H_{cavity} L^3}{\delta EI}\right) \tag{2.22}$$

In the case that the height of the cavity, H_{cavity} is equal to the beam bending amount, δ, further simplifying the result above yields,

$$t_{detach} = (\mu)\left(\frac{1}{h^3}\right)\left(\frac{R^4L^3}{EI}\right) \tag{2.23}$$

This result suggests that the detachment time under no external forces should have some dependance on the elastic modulus and geometric parameters of the conical sucker. The gap height between the two surfaces, h will also be affected by the material and geometric properties of the conical sucker, and determining the gap height for a specific geometry is difficult due to the fact that it requires contact mechanics theory between elastomers and stiff substrates. Hertz contact theory only works for small deformations and therefore would not give a meaningful result. Therefore, we conclude this analysis here, due to the highly coupled nature of the problem and and conclude that experimentation is needed to validate this scaling relationship. We can generally state that Eq. 2.23 implies the following:

$$t_{detach} = f(\mu, h, R, E, H_{cavity}, b) \tag{2.24}$$

where b is the thickness of the cone. Generally, the geometric parameters and elastic modulus of the cone will make the cone have an effective stiffness, k that will effect the detachment time.

Lateral Force

Next, we consider the case of a lateral force acting on the sucker in addition to the separation force. Given assumption 5 that the sucker and substrate come into contact means that the lateral force will have a friction component in addition to the fluid shear component. Research into contact mechanics between elastomers and hard substrates shows that adhesive forces also contribute to this lateral force [30, 29, 35].

Because of the fact that the sucker is highly compliant and in contact with the substrate, the contact mechanics are complex and highly coupled. Persson and Roberts, pioneers in the field of contact mechanics between elastomers and hard substrates, state that the lateral forces are highly dependant on the substrate, the type of elastomer, the fluid and other debris present on the substrate [29, 35]. Additionally, they

state that the friction force should scale with the real contact area, which is difficult to measure in practice [29, 35]. Therefore we point to the work by Persson, Roberts and others for the theory.

Contrary to the lateral force scaling in stefan adhesion, the lateral force between elastomers and substrates depend on more parameters, that are highly coupled. In order to properly determine the lateral between a specific compliant elastomer and a specific substrate, experiments can be performed to give insights into the scaling relationships.

2.4 Experimental Validation of Close-Proximity Suction Using a Compliant Suction Cup

In order to validate some of the relevant scaling relationships derived above for the attachment between a compliant cone and a rigid substrate, experiments were performed using in-house fabricated suction cups. The suction cups were molded using silicone polymers by SmoothOn (USA), using custom designed molds. Three types of experiments were performed to determine the separation force, detachment time, and lateral force scalings. The details of each experiment are in each of the sub-sections to follow.

Experimental Apparatus

A custom, leak-proof tank shown in Fig. 2-9, was designed and fabricated in-house for the experimental apparatus. The tank has a pressure transducer (Nidel Copal Electronics) at the center of the base for cavity pressure measurements that feed data into an arduino microcontroller board, that connects to a computer. The tank also has four bolt holes at the inside corners of the tank to allow for different substrates to be secured onto the apparatus. The tank has an 1/4-28 inch hole for fixing it to an instron machine (Instron, USA). A custom aluminum head fixture was designed and fabricated in-house for attaching different suction cups to it using a 7/8-14 inch

thread (this head is shown in Fig. 2-10. The other side of the aluminum head attaches the the instron machine. The entire setup was designed to be mounted on an instron machine.

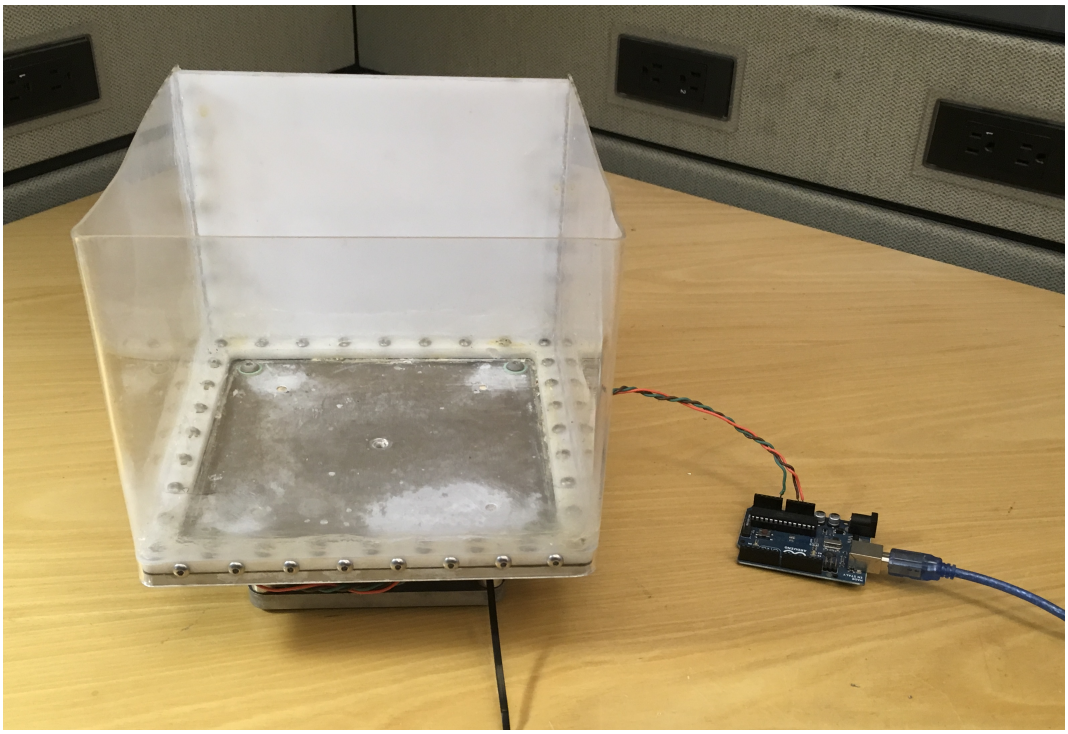

Figure 2-9: Experimental apparatus used for measuring separation force, detachment time, and lateral force on suction-based grippers.

Separation Force Experiments

Separation force experiments were performed to determine the scaling relationship between the separation force and some of the parameters shown by Eq. 2.18. Due to the time it takes to fabricate molds and cast suction cups of varying geometries, the only parameters that were varied for these experiments were the viscosity of the fluid and the separation speed.

Passive suction detachment force is inherently time-dependent because fluid leaks into the cavity of the suction cup, thereby decreasing the cavity pressure. To eliminate the variable of "time" from the problem and isolate the effect of geometry and fluid properties on separation force, experiments were performed on active suction cups

with a 4 Watt diaphragm pump. This lets us assume roughly the same flow conditions for all suction cups and a pressure distribution under the suction cups that doesn't vary with time. The experimental setup is shown in Fig. 2-10.

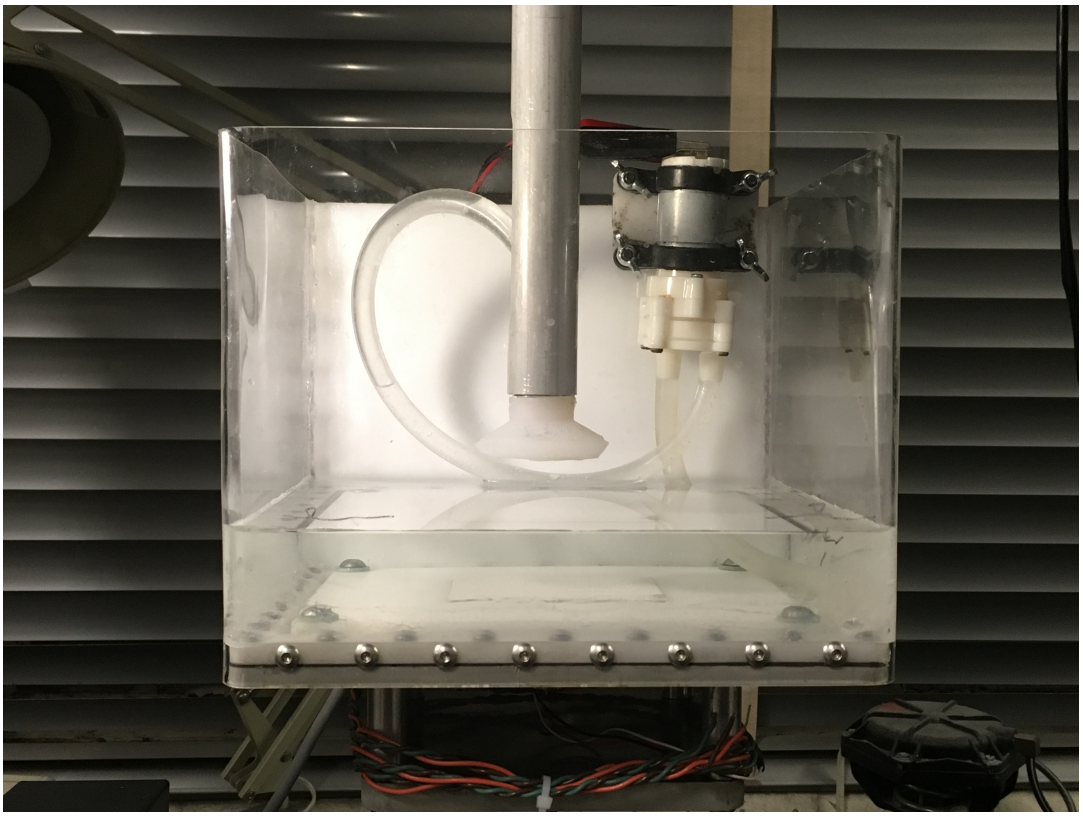

Figure 2-10: Experimental setup to determine separation force on a suction cup.

The separation force normalized by the area of the suction cup when flattened into a disc, A_{disc} is defined as the tenacity, given by:

$$Tenacity = \frac{F_{separation}}{A_{disc}} \tag{2.25}$$

The tenacity vs. viscosity experiments were performed in air and in tap water, using a 50 mm outer diameter (OD) suction cup on a sandpaper substrate of 5 micron macro roughness. We define macro roughness as the mean size of the sandpaper peaks, as opposed to micro roughness which is the roughness of each sandpaper peak. Three experiments were performed for each viscosity. The results of the viscosity experiments are plotted on a log-log plot, shown as points in Fig. 2-11 with a line of

best-fit also plotted.

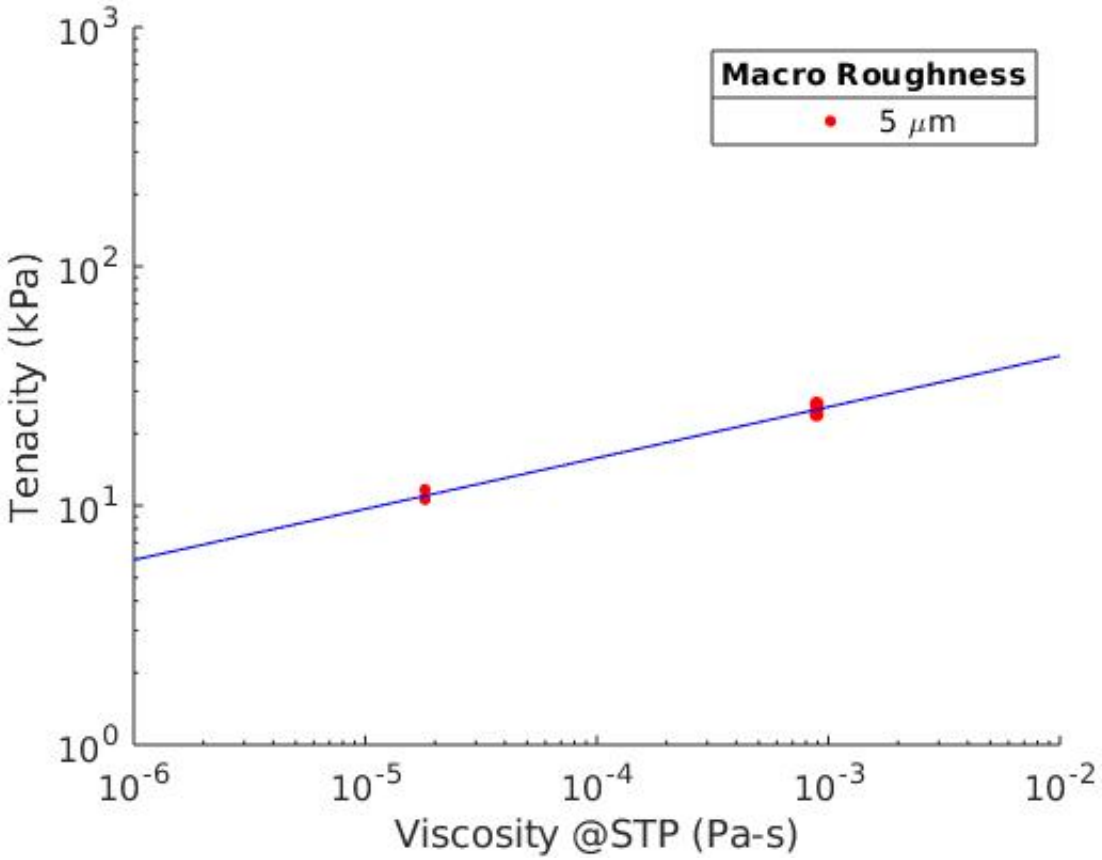

Figure 2-11: Tenacity of 50 mm OD active suction cup vs fluid viscosity.

The results show that the tenacity of a compliant suction cup has a weaker dependence on viscosity compared to that of the geometry in stefan adhesion. A line of best fit shows that the dependence of tenacity of a suction cup on viscosity is:

$$Tenacity \sim \mu^{0.21} \tag{2.26}$$

The tenacity vs. separation speed experiments were performed in tap water, using a 50 mm OD suction cup on a sandpaper substrate of 483 micron macro roughness. Separation speeds of 10, 100, and 500 mm/min were chosen. Three experiments were performed for each separation speed. The results are plotted on a log-log plot, shown in Fig. 2-12 as points with a line of best fit also plotted.

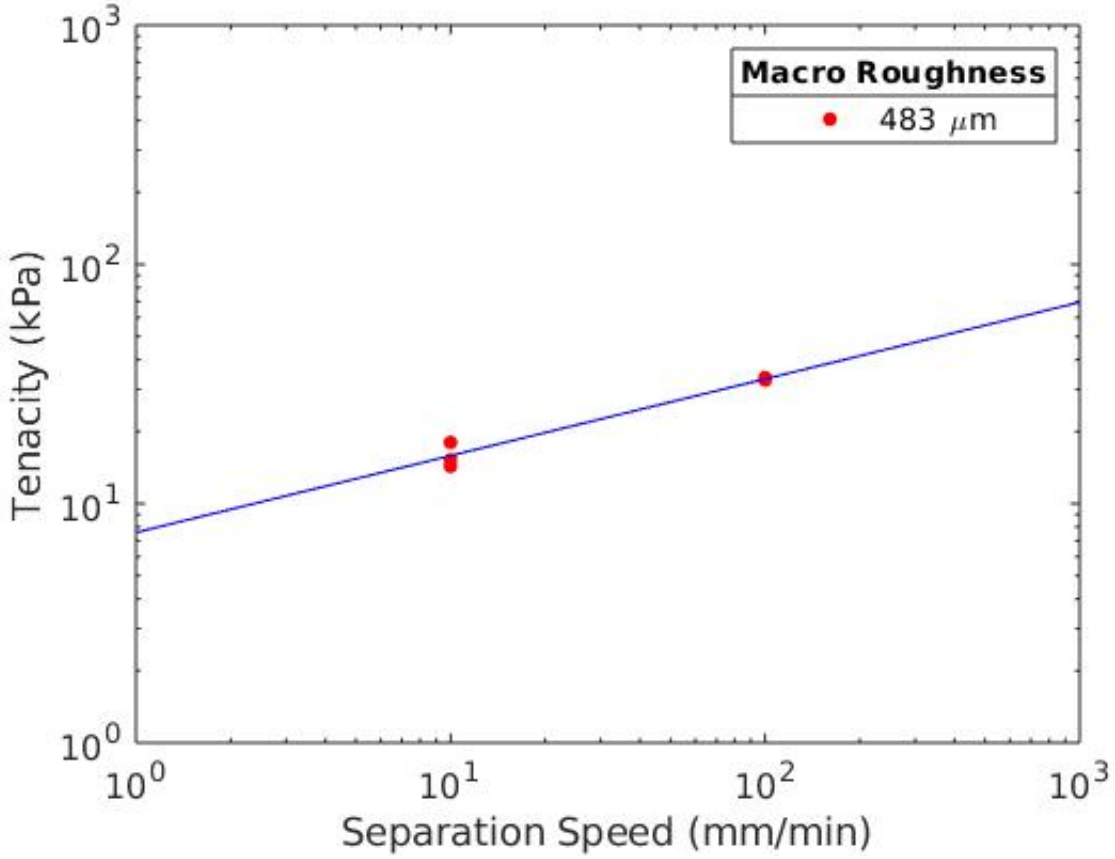

Figure 2-12: Tenacity of 50 mm OD active suction cup vs separation speed.

Similar to the viscosity experiments, the results show that the tenacity of a compliant suction cup has a weaker dependence on separation speed compared to that of the geometry in stefan adhesion. A line of best fit shows that the dependence of tenacity of a suction cup on separation speed is:

$$Tenacity \sim v_{separation}^{0.32} \tag{2.27}$$

The experimental results show the separation force has a significantly weaker dependence on viscosity and separation speed than that of stefan adhesion. A potential hypothesis for the disagreement between the compliant cone geometry and rigid disc geometry could be due to the fact that large deformations in the suction cup allow the suction cup to peel away from the substrate. This peeling effect, causes the suction cup to slide inwards until it has detached. Fig. 2-13 shows an example of this peeling effect when an external separation force is applied to an attached suction cup.

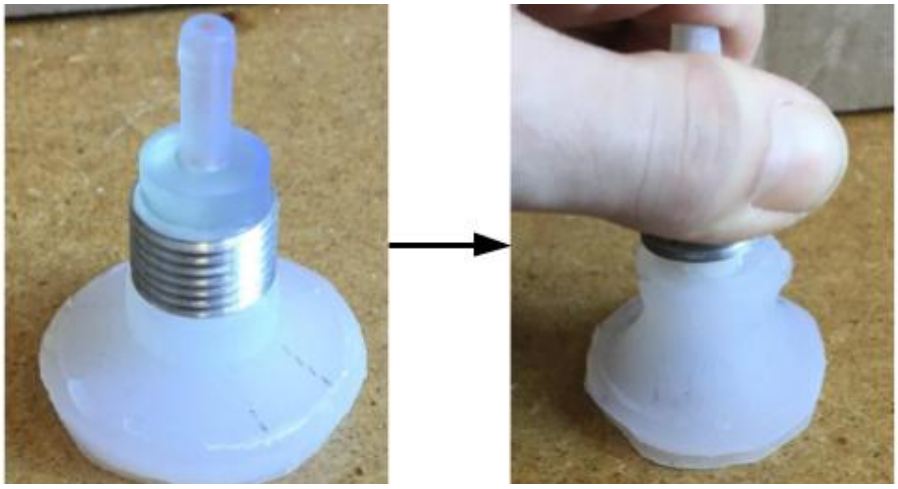

Figure 2-13: Peeling effect of compliant suction cup during detachment.

The results from these experiments are insightful because they inform the design of compliant attachment mechanisms. From a design perspective we now know the detachment force is weakly dependent on the viscosity and separation speed. Furthermore, the elasticity of the suction cup is advantageous in creating an intimate seal with the substrate to slow the leakage of fluid into the cavity, however it is deleterious under the action of an external force because it deforms and peels away from a substrate.

We hypothesize that a multi-material sucker made of a stiff backing layer, and a compliant contact layer would perform better under the action of an external separation force. This is in fact how suction cups such as the one shown in Fig. 2-14 function. Initial experiments show that these suction cups can resist separation forces greater than suction cups without a stiff backing layer. We hypothesize this is due to the stiff backing layer preventing the peeling effect from taking place.

Figure 2-14: Suction cup with a stiff shell for resisting higher detachment forces.

Further experimentation to determine the scaling of the geometry of the suction cup and elastic properties on the detachment force could reveal other insightful relationships. This is left for future work.

Detachment Time Experiments

Detachment time experiments were performed to validate the scaling between detachment time and viscosity of the fluid, given by Eq. 2.23. Since detachment time experiments are non-steady, passive suction cups, designed and molded out of silicone polymer were used for these experiments. The suction cups comprised of a 2.5 mm thick stiff layer of Dragonskin30 (SmoothOn, USA) silicone and a 2.5 mm thick soft layer of EcoFlex 00-10 (SmoothOn, USA) silicone. Experiments were performed with a constant external force acting on the suction cup and with no external force, both in air and in water. Experiments were done in the same experimental apparatus as the detachment force experiments. The experimental setup is shown in Fig. 2-15.

No External Force Case

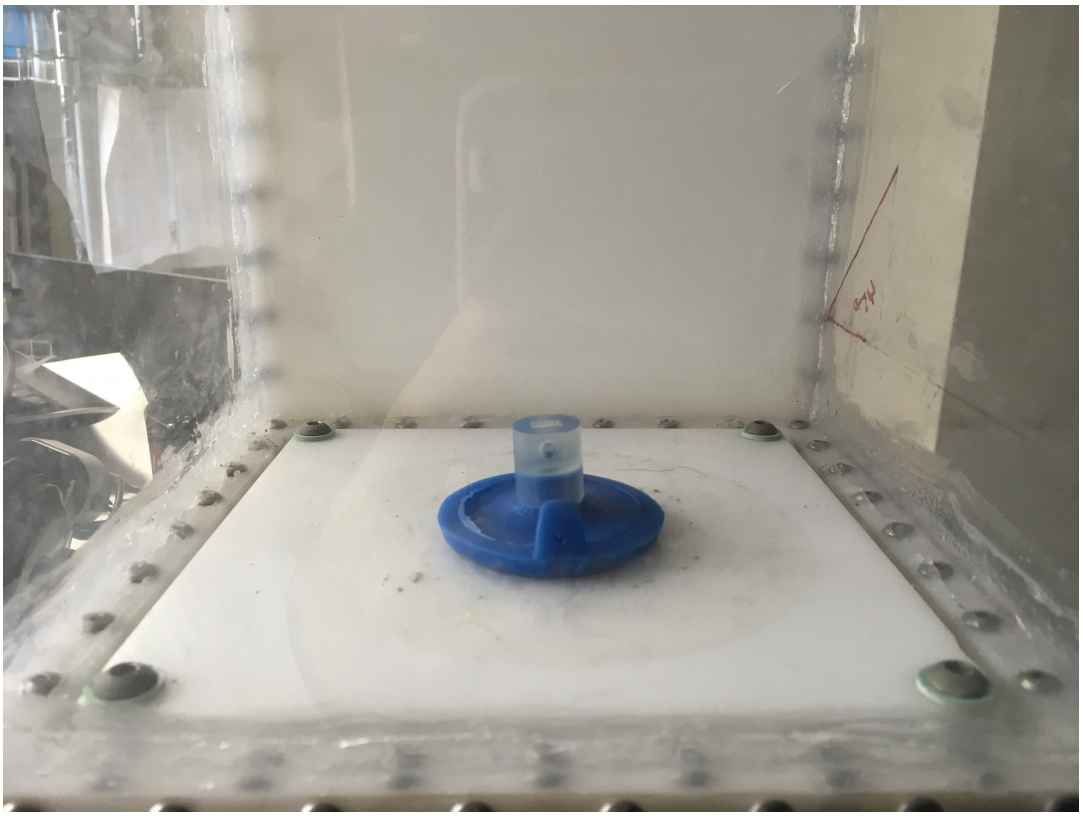

Figure 2-15: Experimental setup to determine detachment time of a suction cup with no external forces.

These experiments were performed using a 50 mm OD suction cup on a 165 micron macro roughness sandpaper substrate. Ten experiments were performed in air and only three experiments were performed in water, due to the long duration of the water experiments. The results are plotted as points on a log-log plot, shown in Fig. 2-16, along with a line of best fit.

These results show that the detachment time of a compliant suction cup has a strong dependence on viscosity of the fluid it is immersed in. A line of best fit in the data shows that the dependence of detachment time on viscosity is:

$$t_{detach} \sim \mu^{1.2} \tag{2.28}$$

These results are significant because it allows for a way of predicting detachment time for a specific geometry suction cup, on a specific substrate and immersed in a specific newtonian fluid by simply doing an in-air experiment. In practice, it is

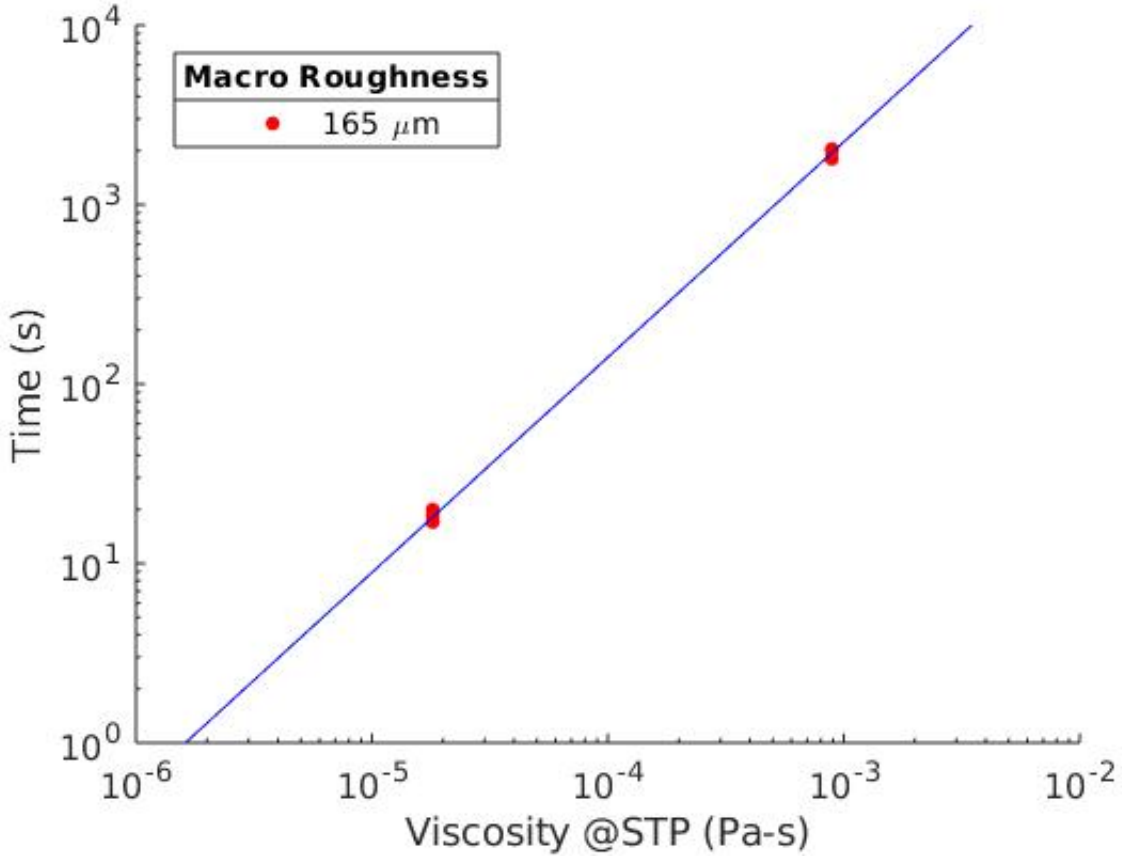

Figure 2-16: Detachment time of a 50 mm OD suction cup vs fluid viscosity.

difficult to predict exactly how much time it would take to detach without doing an experiment because the time depends on the elastomer-substrate interaction, which is difficult to model, as discussed earlier.

Preliminary experiments with a constant step external separation force show that the experiments also agree with the scaling given by Eq. 2.20 however these results will be presented in a future publication. Given the experimental data, we hypothesize, that an experiment performed in-air would accurately still predict the detachment time in another fluid under the same geometric and dynamic loading conditions.

It is also important to note that the experiments show that even on a relatively smooth surface, of same order roughness as ship hull [39] a 50 mm OD suction cup can stay attached for approximately 18 minutes. Using initial experiments done in air on a glass substrate with no external forces we predict that the suction cup should

be able to stay attached to the same substrate underwater on the order of months.

Lateral Force Experiments

Due to existing work by Miyake et. al. on the lateral force resistance of suction cups, detailed lateral force experiments were not carried out in this thesis [27]. From Miyake's work we conclude that the lateral force on a suction cup is at least a function of the fluid viscosity, μ, the horizontal sliding velocity, $v_{horizontal}$, and the cavity pressure, ΔP_{cavity}.

$$F_{lateral} = f(\mu, v_{horizontal}, \Delta P_{cavity}) \tag{2.29}$$

Miyake's results show that the lateral force of a suction cup is proportional to the the cavity pressuse, and horizontal sliding velocity but inversely proportional to viscosity of the surrounding fluid. Initial Experiments performed with a 50 mm OD suction cup on a smooth (<10 micron roughness) substrate confirm Miyake's results. Most importantly, experiments we did in water and in silicone oil which was two orders of magnitude more viscous than water, confirms that in the presence of a more viscous fluid the friction force decreases.This experimental setup is shown in Fig. 2-17.

This result introduces a tradeoff in suction-based gripper design. Higher viscosity fluids, which help in achieving higher tenacities and significantly higher detachment times are in fact deleterious to lateral forces.

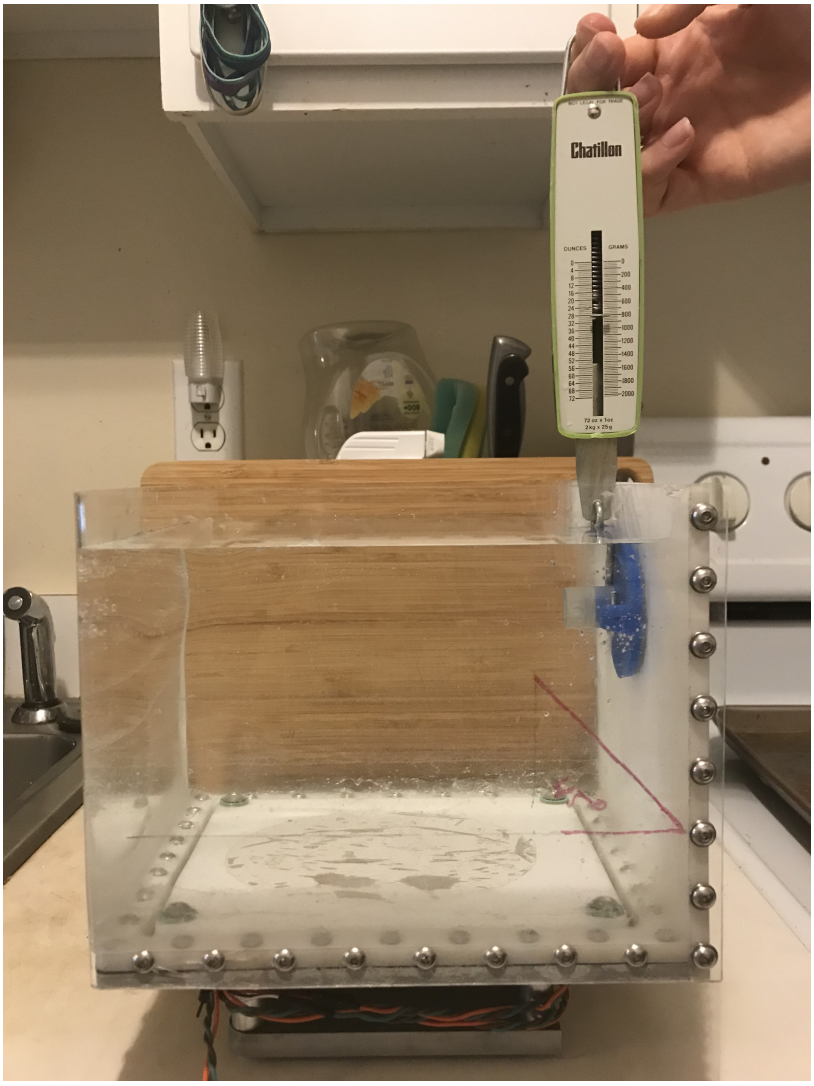

Figure 2-17: Experimental setup to determine lateral force on a suction cup.

Chapter 3

Exploration of Suction-Based Attachment & Locomotiom Mechanisms

The model and experiments presented in Chapter 2 give us a better understanding of the fundamental physics behind close-proximity suction-based attachment, and how the detachment force, detachment time, and the lateral force of compliant suction-based grippers scale with physical parameters. Using this understanding, we can begin to explore different attachment mechanisms for the application of UVHC. As we will later show, attachment systems are generally coupled with locomotion mechanisms for crawling robots. In this chapter, we aim to explore some of these coupled attachment and locomotion mechanisms for crawling applications.

First, we review existing devices and animals that rely on suction-based attachment to feed, mate and survive to learn about the functionality and limitations of existing devices and how nature has optimized and evolved for suction-based attachment. Then, we present some new mechanisms that were fabricated in this thesis based on findings in literature. In no way is the following information on attachment and locomotion systems for vessel hull cleaning exhaustive, however trends discovered in literature review are presented to demonstrate the current state of the technology.

3.1 Lessons from Nature: How Nature Attaches and Moves

Research shows that underwater animals that remain stationary throughout their lifetime such as mussels, oysters, and barnacles rely on permanent attachment mechanisms [52, 51]. These animals secrete organic adhesives based on dopamine, that allows them to form permanent bonds [52]. Comparatively, mobile underwater animals that rely on attachment to feed, mate, and survive from predators such as remoras, lampreys, octopi, northern clingfish and waterfall climbing gobys, shown in Fig. 3-1 use suction to attach to surfaces, and limbs or fins to move by pushing on the water to generate thrust forces.

Figure 3-1: Examples of underwater animals that rely on suction for attachment and in and in some cases, locomotion.

We hypothesize that one of the reasons underwater animals rely on suction-attachment is because separation forces and detachment time scale with viscosity of the surrounding fluid. This was experimentally validated in Chapter 2. Since the viscosity of water is two orders of magnitude higher than that of air, it makes suction-based attachment more effective in water, and may explain one reason why some in-air and on-land animals such as snails secrete viscoelastic fluids locally to

attach to surfaces [16].

On the macro scale it is evident that underwater animals such as the ones in Fig. 3-1, have external morphological similarities in their suction organs, such as being round shaped and compliant. Research shows that on the micro scale the suction organs of these animals have different morphological features and complex structures of various layers of tissue with different mechanical properties [15, 5, 10, 46]. These morphological differences allow the animals to specialize in attaching to certain substrates, resisting detachment forces or attaching and detaching reversibly for rapid locomotion in order to feed, mate and survive from predators [15, 5, 10, 46].

One similarity observed over numerous underwater animals that rely on suction is that their suction organs contain a characteristic soft contact layer with a low elastic modulus on the order of $10^3 - 10^4$ Pa, and a characteristic stiff backing layer with an elastic modulus at least twice higher than that of the soft layer. For example, octopus suckers contain a soft contact layer called the infundibulum that has an elastic modulus of order 7×10^3 Pa, and a stiff outer layer called the acetabulum that has an elastic modulus of order 2×10^4 Pa.

Using these findings, research has attempted to immitate the suction organs of animals by inventing active and passive bio-inspired suction mechanisms [13, 50, 24, 18]. These bio-inspired suction-based mechanisms, are generally made of elastomers and are comprised of a compliant contact layer and a stiff shell or backing layer. In the following sections, we explore some implementations of suction-based attachment and locomotion mechanisms for underwater crawling applications and present some reversible suction-based attachment mechanisms of our own for the application of UVHC and inspection.

3.2 Suction-Based Attachment and Locomotion with Limbs

Attachment and locomotion with limbs is found in numerous in-air and on-land robots, however there have not been numerous limbed robots for underwater crawling applications. We hypothesize that the lack of realized limbed robotic devices for underwater crawling applications is due to the multiple degrees of freedom (DOFs) presented by limbs. Multiple DOFs is usually associated with multiple actuators, which increases the technical complexity of controlling the actuators.

As a result, underwater crawling robots currently in practice, mainly rely on magnetic, thrust, or suction-based mechanisms for attachment and locomotion. For reference, [11] has a non-exhaustive list of crawling robots in industry primarily used for cleaning and inspection of vessel hulls. Despite their complexity, there have been a limited number of limbed robots that have been proposed or fabricated and tested in literature for the application of vessel hull cleaning. Next, we will explore two such robots, one that uses distant suction and one that uses close-proximity suction for attachment and locomotion.

Distant Suction

In 2013, Souto et. al. presented a limbed robot called Lappa, that was fabricated, and tested for the application of in-port recreational boat hull cleaning, shown in Fig. 3-2 [42]. The under-actuated, tethered robot has a total of 5 DOF and uses two DC motors with impellers for creating suction and a 3 DOF linkage arm to move in zig-zag patters along the hull. The impellers can be in the reverse direction to create thrust in the case where the robot needs to detach and resurface. Experiments showed that the robot can attach with over 900 Pa of pressure at a 1 cm proximity to the hull surface. There was no information reported on the power consumption of the robot, however based on the size of the actuators we predict the power consumption of each motor is in the few hundreds of Watts to 1 kW range.

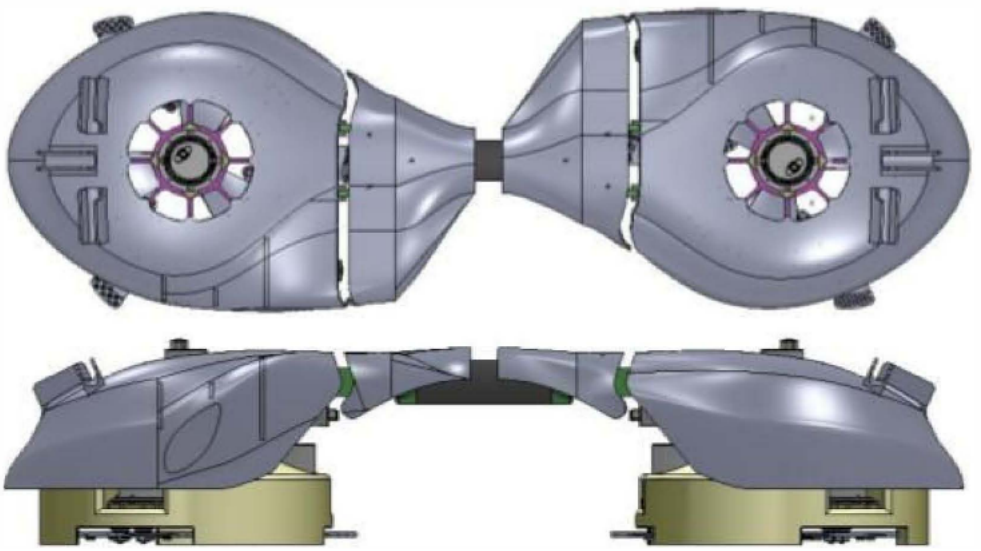

Figure 3-2: Concept of a limbed hull cleaning crawler robot proposed by Souto et. al. (adapted from D. Souto).

The reason we highlight the robot in Fig. 3-2 is because, due to it's under-actuation, it only requires two actuators to attach and move. This robot represents one of the simplest limbed robots that may be achievable for underwater crawling applications, yet it only attaches to surfaces with 900 Pa of pressure, which would preclude it from being viable for the UVHC application.

Close-Proximity Suction

Similarly, in 2013, Albitar et. al. presented a concept of a tethered, limbed crawling robot, shown in Fig. 3-3 for the application of underwater stationary or underway ship hull cleaning [2]. The proposed concept has a total of 12 DOF and uses two motors for actuating the main linkages at the apex of the triangle-like structure, and actively actuated suction cups in order to reversibly attach and crawl in a biped-like pattern. The authors claim the robot is simple, yet it uses multiple actuators and pumps for actuating the attachment and locomotion systems. No analysis was performed to determine the power consumption of the robot.

As evident by these robots, limbed robots have numerous DOFs and are complex to control and actuate for locomotion. In the case of active distant suction-attachment the motors to drive impellers consume large amounts of energy to maintain under 1000

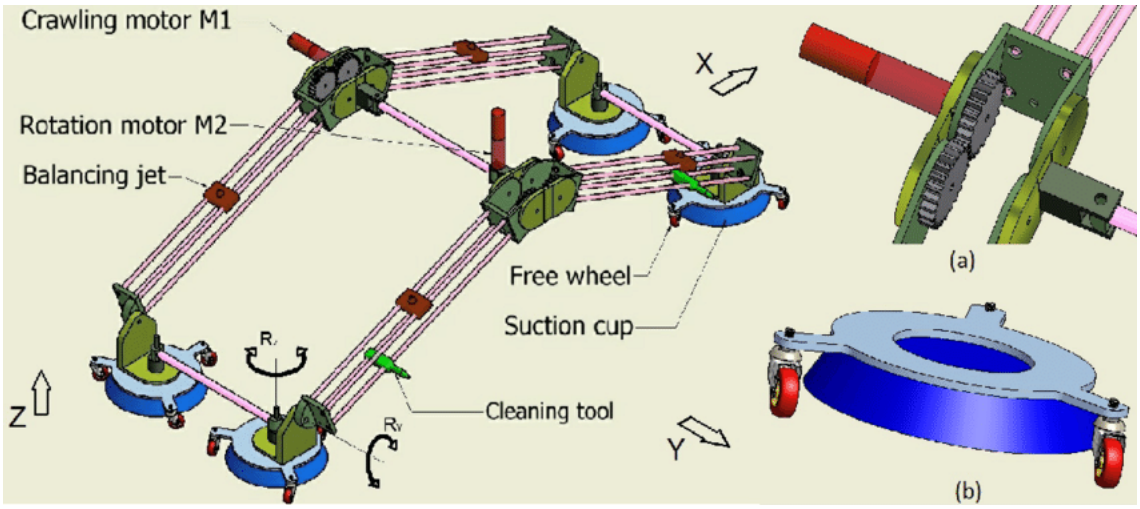

Figure 3-3: Concept of a limbed hull cleaning crawler robot proposed by Albitar et. al. (adapted from H. Albitar).

Pa of attachment pressure. Despite these challenges, limbed robots may be realized for the application of UVHC, but at a higher cost. The cost of these robots may make them cost-prohibitive, as it is a well-known fact that cost increases with increasing complexity.

If a robust limbed hull crawler could be realized for the application of UVHC, where detachment is catastrophic, the most critical module of such a device would be the suction gripper. From an engineering perspective, this allows us to decouple the attachment and locomotion subsystems and turn our focus on designing an effective gripper that can later be placed on a limb.

3.2.1 Existing Suction-Based Grippers

Among existing suction-based grippers and attachment systems found in literature, various ones for attaching to relatively flat and smooth surfaces, similar to a vessel hull, are selected and outlined in Table 3.1 below along with tenacity and lateral stress information. Lateral stress is defined as the lateral force normalized by the gripper area. Information that was missing or not reported is marked with a dash.

As evident by the reported figures, suction-based grippers have relatively high

Device Name	**Company / Institution**	**Tenacity (Pa)**	**Lateral Stress (Pa)**
Clingfish-inspired passive suction cup	Research, Ditsche et. al. [13]	7×10^4	-
Remora-inspired active suction disc	Research, Wang et. al. [50]	5.8×10^4	4.8×10^3
High friction active suction cup	Commercial Product, PIAB [31]	3.3×10^4	8.8×10^4
Octopus-inspired dielectric elastomer suction cup	Research, Follador et. al. [18]	6×10^3	-
ZPD active suction unit	Research, Shi et. al. [41]	1.8×10^4	-

Table 3.1: Examples of existing suction-based grippers and their reported tenacity, and lateral stress.

tenacity and lateral stresses, which makes them ideal for the UVHC application.

3.2.2 New Suction-Based Grippers Explored in this Thesis

As Table 3.1 shows, there is a vast diversity of suction-based grippers ranging from passive grippers to active grippers with multiple DOF and multiple actuators. Using this information, we designed and fabricated proof-of-concept prototypes of two new grippers, with the design philosophy of keeping them as simple as possible and requiring minimal energy, while still able to reversibly attach and detach rapidly for the application of UVHC with a limbed crawling robot. To consume minimal energy, all of the devices presented below make use of close-proximity suction.

Active Suction Cup with Inner Cavity Expansion

This concept, shown in Fig. 3-4 uses a back-drivable pump to attach and detach to a substrate and a piston on a threaded rod driven by a motor to expand the inner cavity volume and generate higher suction forces than would be generated by the pump alone. The threaded rod allows for a large mechanical advantage in expanding

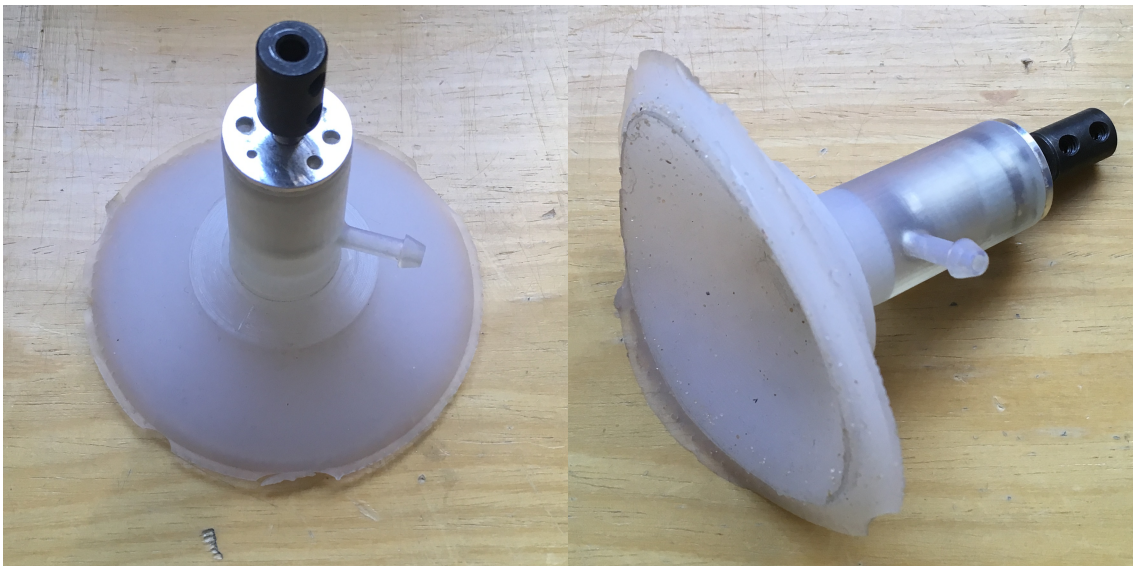

((a)) ((b))

Figure 3-4: Prototype of active suction cup with inner cavity expansion.

the volume, and thus a requires a smaller actuator that consumes minimal energy to drive the threaded rod. The actuator used for expanding the volume was a 5 Watt DC geared motor.

The gripper consists of a stem overmolded with silicone in the shape of a suction cup. The stem has an aluminum chamber adhered to it for allowing the piston to slide along the chamber walls. The threaded rod has one side attached to the piston and the other side to a shaft coupling that couples to the DC gear motor (not shown). Two threaded rods (not shown) that are attached from the motor to the aluminum chamber, prevent the motor from spinning in place when actuated. The gripper was not thoroughly tested for tenacity and lateral force experiments however preliminary tests showed that it held with a larger tenacity than the simple suction cups experiments performed in Chapter 2.

Jamming Granular Material Gripper with Active Suction

This concept, inspired by the universal jamming granular grippers for gripping any-shaped object [8], uses two pumps, one for evacuating the fluid out of the grain bladder to initiate jamming and the other for generating suction. The two pumps

consumed a total of 8 watts when actuated continuously.

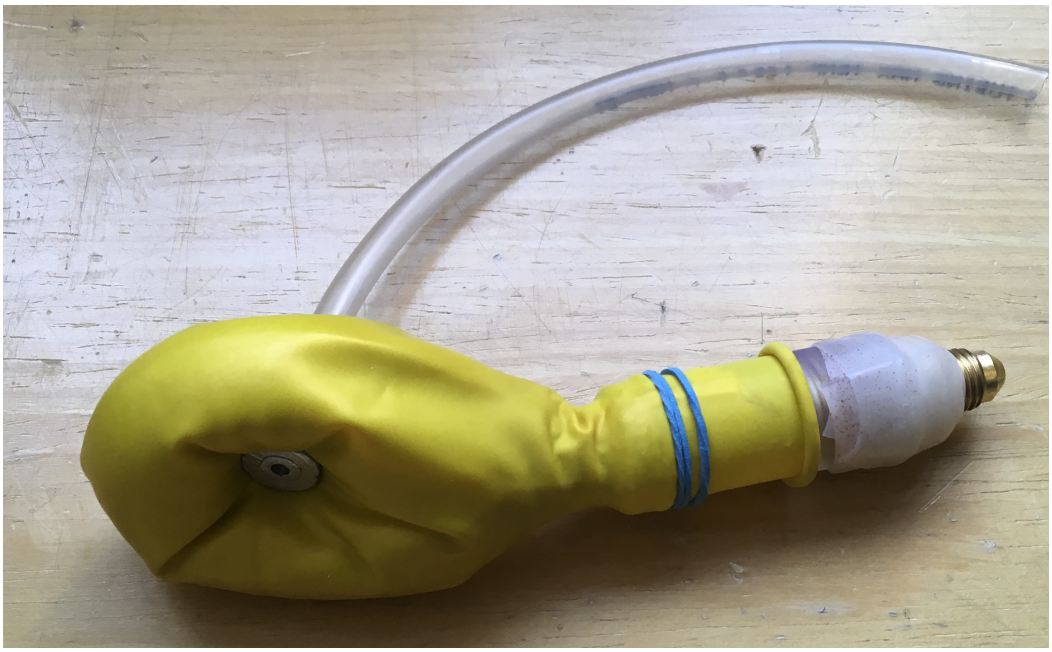

Figure 3-5: Prototype of jamming granular material gripper with active suction.

The gripper consists of a sand filled bladder made of a latex balloon, punctured with a hole in the center for an inlet port for the suction pump. The throat of the balloon is used for evacuating fluid from the grain bladder. Attempts to cast a soft silicone layer over the latex balloon failed due to the difficulty in adhering polymers to latex. When tested on a flat surface, the device did not perform as expected. We hypothesize that this is due to the jamming of the grains. While jamming is critical to attaching to surfaces with three-dimensional (3D) protrusions, it is deleterious to attaching to flat surfaces. This is due to the fact that elastic energy cannot be stored in the granular material in the jammed state, thereby emulating a rigid gripper, resembling the stefan adhesion geometry shown in Chapter 2.

3.3 Suction-Based Attachment and Locomotion with Treads/Wheels

Attachment and locomotion robots that utilize wheels or treads are ubiquitously found in numerous on-land and underwater applications [17, 11]. Wheels or treads are a mechanically simpler way of locomotion due to the fact that a minimum of two actuators are required in order to differentially drive and make turns.

As a result, numerous underwater robots in practice such as in-port vessel hull cleaning and inspection robots utilize wheels and treads with permanent magnets, thrusters, or suction for attachment and locomotion [11]. Next, we will explore two of these devices that use suction-based attachment and locomotion technology: an underwater inspection robot that uses distant suction and an in-air inspection robot that uses close-proximity suction. These devices show the variation in the current state of the technology.

Distant Suction

The Vectored Little Benthic Crawler (vLBC) by Seabotix, shown in Fig. 3-6 is an underwater vessel hull inspection robot that uses a patented vortex suction technology to actively attach to surfaces and treads to move [45]. The 35 kg robot can attach to flat surfaces with 210 N of force and 25 cm clearance [45]. This force normalized by its area footprint yields an attachment pressure of just under 900 Pa. It has 6 thrusters for maneuvering when it is not attached to a surface. There is no information reported on the power consumption of the device, however similar underwater inspection robots consume power in the hundreds of Watts range [11].

Robots such as the vLBC are relatively light, compact, and simple in their operation, but their attachment pressures of order 10^3 Pa preclude them from being a viable solution for the UVHC application.

Close-Proximity Suction

There were no close-proximity suction robots that use wheels or treads found in

Figure 3-6: vLBC, underwater inspection robot by Seabotix.

industry for underwater application. We hypothesize that this is due to the fact that fouled surfaces present a challenge for a close-proximity suckers. In order for close-proximity suction to function effectively on rough, fouled surface, the sucker must be highly compliant in order to morph into the shape of the substrate in order to form close-proximity attachment. In our research however, we found an in-air inspection robot that uses close-proximity suction and treads to move.

Robotic Crawler, shown in Fig. 3-7 by Invert Robotics, a new Zealand-based start up company, is a beverage and chemical tank inspection robot that uses suction cups that slide along smooth, flat surfaces to maintain attachment, and elastomer treads to move [22]. The company claims that the 5 kg robot consumes a total of 200 W in order to attach with both active and passive suction cups [22]. There is no information on the amount of pressure the robot can attach with. From images of the robot (Fig. 3-7) it appears that the pneumatic hoses lead to a vacuum system that is external to the robot. This implies the robot can theoretically attach with a pressure difference equal to that of what the vacuum pump can generate. There is no

information on the lateral forces the robot can resist but based on the application, we can assume that it can support its own weight from sliding with the elastomer treads.

Figure 3-7: Robotic Crawler, in-air inspection robot by Invert Robotics.

Robotic Crawler shows some promise for use in the UVHC application, however there is a significant downside that would preclude such an attachment system for use in hull cleaning. As claimed on Invert Robotics' website, the robot only attaches and moves on smooth surfaces [22]. A vessel hull, which has weld lines, potential fouling and other protrusions [37] would pose serious challenges to sliding suction cup technology. Therefore, we conclude that this attachment technology would not be feasible for use on a robot for the UVHC application.

Based on thorough research into existing attachment and locomotion technologies and the material presented above, we can conclude that all of the existing concepts, technology and robots on the market do not show promise of working for the application of UVHC. The overall system complexity, insufficient attachment pressure, or large energy requirements in order to generate sufficient attachment pressures preclude the existing technology from working for UVHC.

3.3.1 New Concept: Continuous Peeling of Passive Suction Cups on a Tread

The presented research has shown that grippers alone can be complex and actuating multiple active grippers in a limbed robot adds significant complexity to the overall system. Additionally, current attachment and locomotion technologies have significant disadvantages that preclude them from being used in a hull crawler for UVHC. Despite its limitations on maintaining attachment and locomotion on a ship hull, only one device, Robotic Crawler by Invert Robotics shows the most promise towards meeting the technical requirement for the application. This robot uses close-proximity suction with suction cups to maintain attachment using minimal power input (200 W). This low energy cost of attachment is highly desired for UVHC application.

In Chapter 2 we presented experiments that show that 50 mm OD, passive suction cups can stay attached on smooth (<150 micron roughness) surfaces up to 18 minutes and predicted them to last on glass-like surfaces on the order of months, without the action of an external detachment force. Additionally, we confirmed findings in research, that they to maintain attachment pressures higher than 25 kPa and high lateral forces on smooth substrates. These findings conclude that a passive suction cup may be ideal for this application.

Here, for the first time, we present a new concept for low-power, reversible attachment and locomotion using passive, bio-inspired suction cups on a tread. The bio-inspired suction cup's long attachment duration underwater, are ideal for applications where a robot needs to stay attached while actively moving. The concept, shown in Fig. 3-8, relies on the *continuous peeling action through tread curvature* to engage and disengage multiple bio-inspired suction cups to and from a surface, while moving along the surface.

A detailed, side-view of the concept is shown in Fig. 3-9. As shown, each suction cup is coupled to the tread by a rigid member. The distance between two adjacent suction cups, Δ_1 increases to Δ_2 in the curved part of the tread, and therefore causes the suction cups to elastically peel back in order to either attach or detach to the

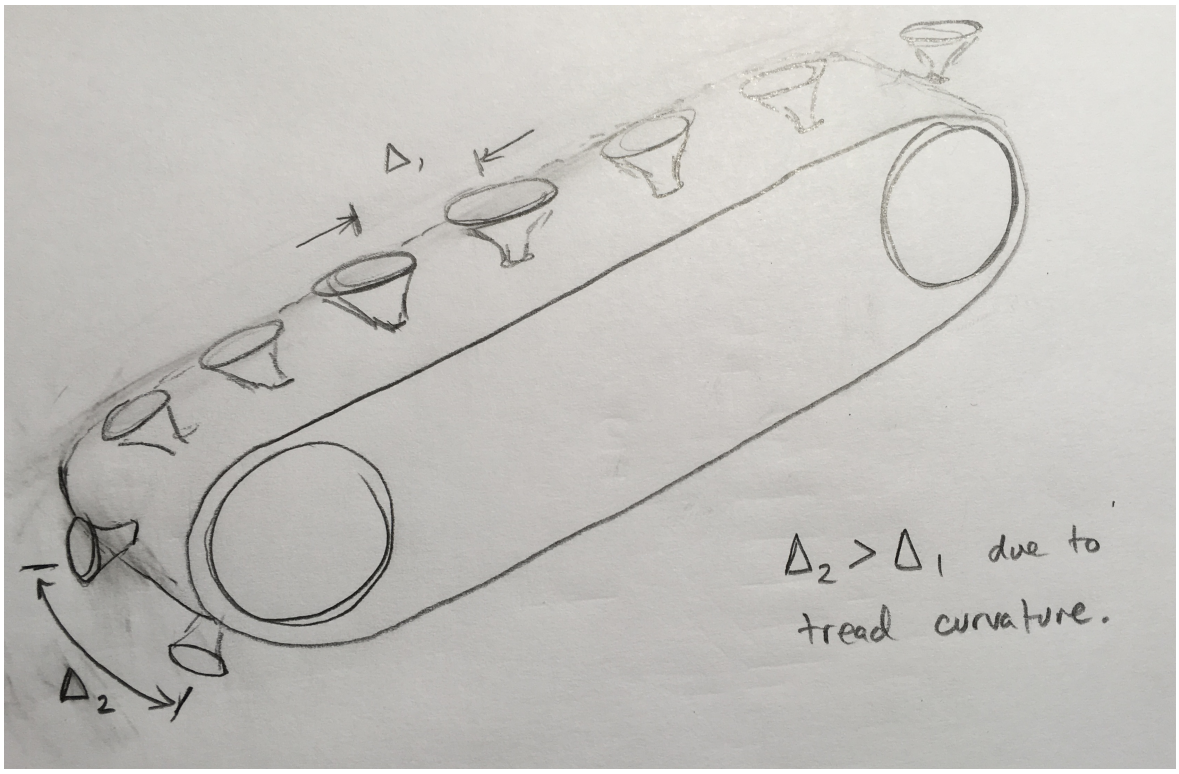

Figure 3-8: Concept sketch of continuous peeling of suction cups on a tread.

substrate. By varying the length, H that the suction cups protrude from the tread, the amount of deformation can be controlled. The change in arc length given by Eq. 3.1, can be used to design the mechanism so that it peels the suction-cups by an amount that will not cause material failure.

$$\Delta_2 - \Delta_1 = H\theta \tag{3.1}$$

The concept could be used in energy constrained underwater environments as the primary mode of attachment, supplemented by an active system in the case of unanticipated detachment forces. In Chapter 4 a proof-of-concept prototype of this concept is presented along with the design, fabrication and testing details.

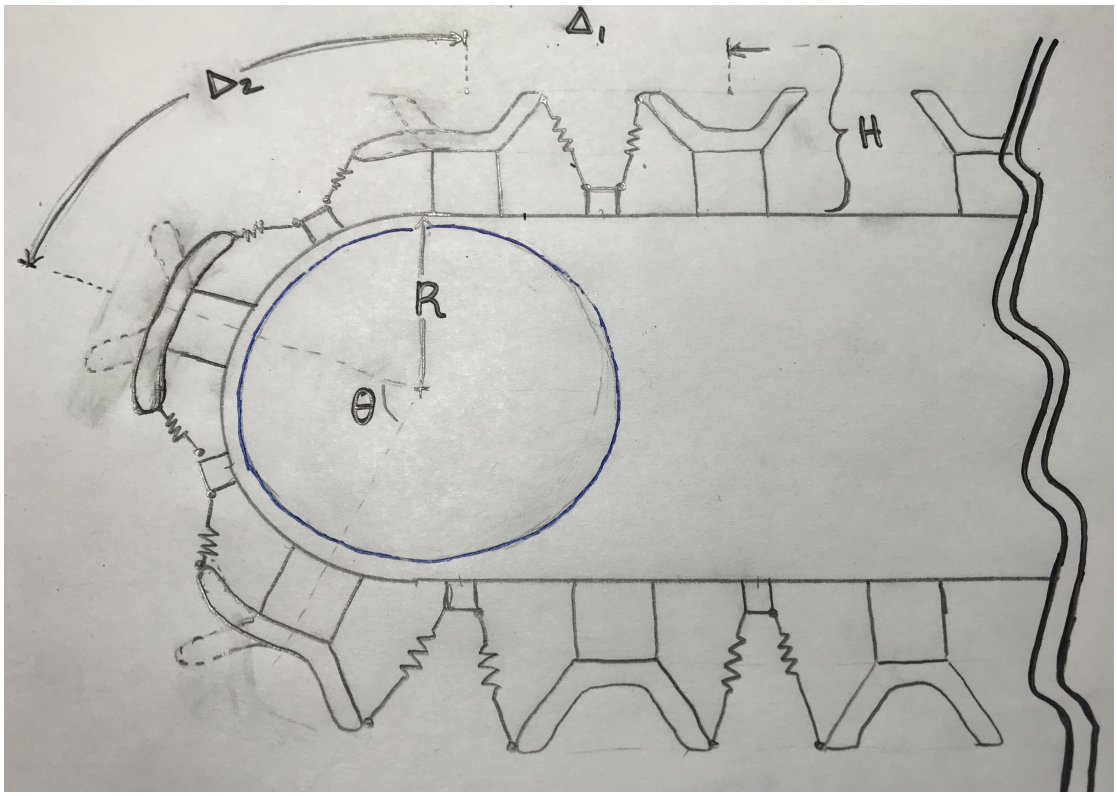

Figure 3-9: Side-view of continuous peeling of suction cups on a tread concept.

Chapter 4

Design of a Scale Model Robot to Demonstrate Continuous Peeling of Passive Suction Cups on a Tread

Using key insights from analysis and experimentation of suction-based attachment and exploration of previous work done on suction-based grippers and attachment and locomotion systems, a new attachment and locomotion concept was presented in Section 3.3.1. The concept makes use of the *continuous peeling action through tread curvature*, whereby the continuous peeling of bio-inspired suction cups on a tread facilitates locomotion on a surface while remaining attached with minimal input energy.

The mechanism could be implemented on underwater robots in applications that are energy or power constrained. This can help reduce the volume and weight of a robot from batteries and bulky actuators. In the application of UVHC, this mechanism could serve as the primary attachment system because it does not require large energy input, other than the energy required to actuate the treads. An active attachment system would supplement this mechanism and would turn on in the case of an emergency, to avoid catastrophic detachment.

4.1 Concept Overview & Operation

A proof-of-concept prototype of the concept, shown in Fig. 4-1 was designed, fabricated and tested and the methodology and results are presented below.

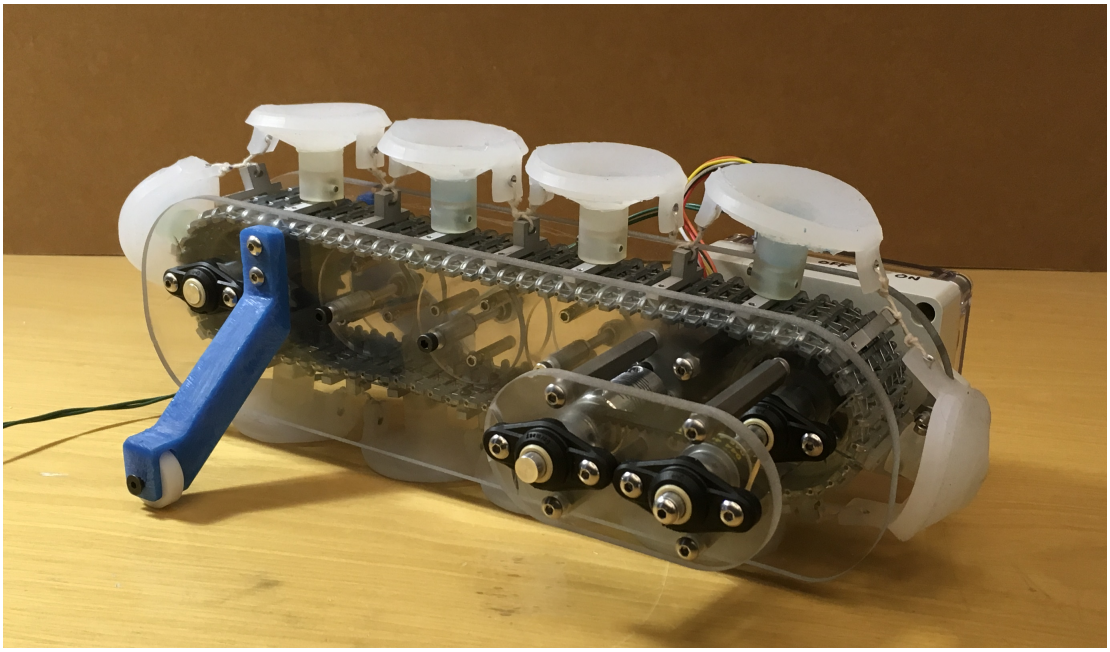

Figure 4-1: Proof-of-concept prototype.

The goal of the proof-of-concept prototype was to show the feasibility of passive close-proximity suction-attachment using the continuous peeling of passive suction cups through tread curvature. The set of functional requirements that the prototype was designed to meet are outlined in Table 4.1. The functional requirements serve to guide the design of a prototype that can be tested in the laboratory setting in bench-top level experiments. Therefore, a single tread was designed and fabricated to save time and resources.

Operation

In its basic operation, a single actuator drives the tread, which moves the device in a straight line. As the robot moves, it begins to attach to a substrate by the peeling of each suction cup that comes into contact with the substrate. With each successive suction cup that comes into contact with the substrate, a suction cup

No.	Requirement	Requirement Details
1	Continuous Attachment during locomotion	Once attached, the robot must remain attached while moving and while stationary
2	Power Budget	Robot must be able to be operated using a desktop power supply
3	Speed Requirement	Robot drive train must be designed so the robot moves at speeds up to 5 cm/s
4	Corrosion Resistance	Use parts to minimize corrosion and galvanic corrosion that main occur during testing in the presence of or splashing of water

Table 4.1: Functional requirements of scale model attachment & locomotion robot.

detaches from the substrate at the other end of the tread, thereby allowing the robot to move without impediment. The device does not require initial manual attachment on horizontal or declined surfaces due to its weight acting in the direction of the attachment. On inclined surfaces greater than about 30 degrees, the device requires manual attachment to the surface. Manual attachment can be done by pressing the device against the surface to engage the suction cups adjacent to the surface.

4.2 Design

A computed aided design (CAD) model of the system was created using SolidWorks (Dassault Systemes, France). The model, with each subsystem labeled is shown in Fig. 4-2. The peeling couplers and driving belt are not shown in the CAD model due to the difficulty in modeling those items. The device weighs slightly over 2 kg, measures 38 cm in length x 21 cm in width x 14 cm in height, and consumes 10 W of continuous power on horizontal surfaces.

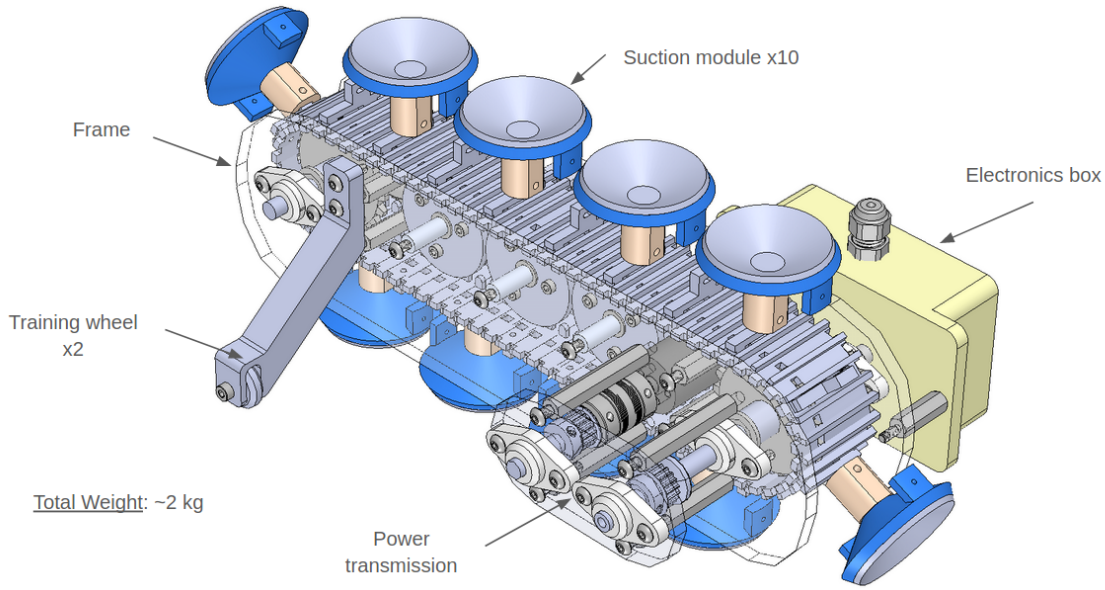

Figure 4-2: CAD model of prototype.

4.2.1 Frame

The frame, shown in Fig. 4-3, consists of three 6.3mm thick polycarbonate sheets fixed together with 50mm length stainless steel standoffs. Each of two training wheels is composed of a single structural member rigidly attached to the polycarbonate sheet with two bolts, and an idling acetal wheel that spins freely on a shaft. The frame was primarily fabricated out of plastic components and stainless steel fasteners and standoffs in order to meet the corrosion resistance functional requirement (No. 4). The training wheels prevent the robot from tipping to either side due to the fact that the center of gravity is above the points of contact.

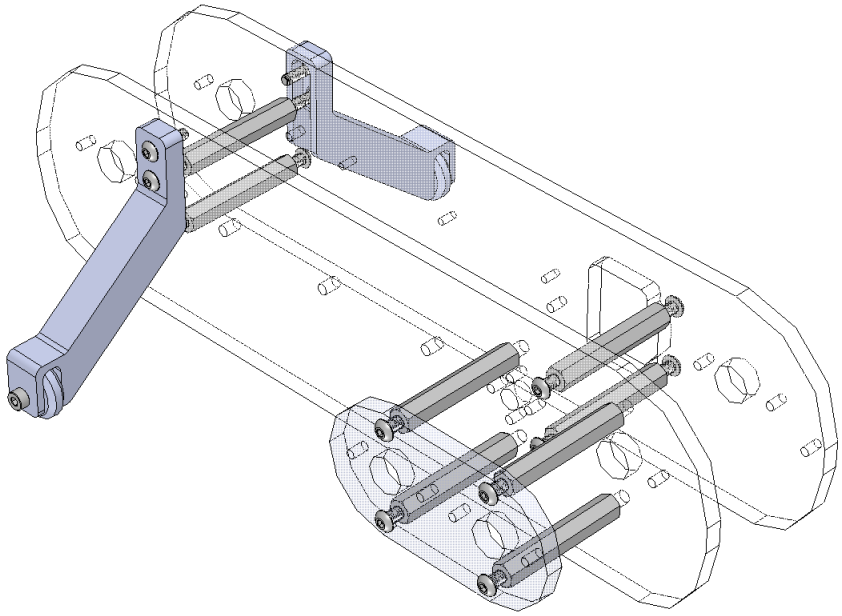

Figure 4-3: CAD model of frame.

4.2.2 Power Transmission

The power transmission system shown in Fig. 4-4 consists of a single 9-24 Volt direct current (DC) gearhead motor that is coupled, using a commercially available coupling, to a shaft. The shaft transmits torque to an adjacent parallel shaft through an approximately 1:1 reduction ratio using an HTD toothed belt-pulley system. The adjacent shaft transmits torque to a dual sprocket that rotates the tread links. Three, acrylic idler rollers along the length of the tread prevent the tread from sagging. All of the rolling elements with the exception of the idler rollers rotate on panel mounted nylon spherical bushings that compensate for any misalignments between the frame plates. The power transmission system was designed to meet the robot speed functional requirement (No. 3) by designing the belt-pulley reduction ratio approximately 1:1 and the gearhead motor reduction ratio 75:1.

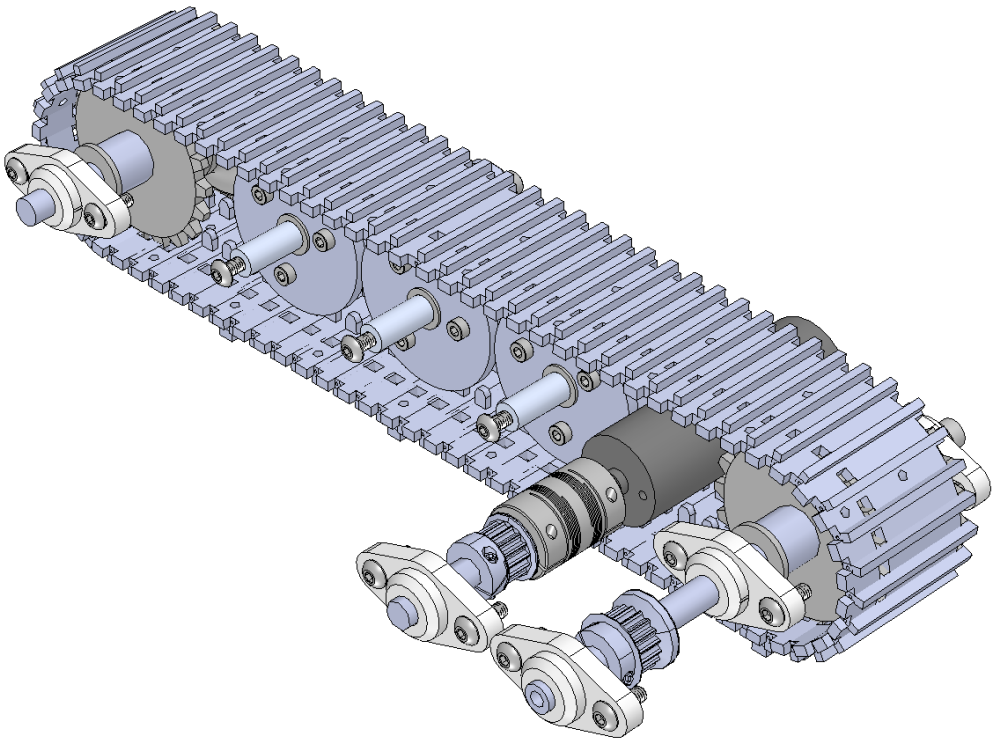

Figure 4-4: CAD model of power transmission, with the driving belt not shown.

4.2.3 Attachment and Locomotion System

The attachment and locomotion system consists of ten silicone bio-inspired suction modules coupled to a post that is mounted to the tread using two bolts. The bio-inspired suction modules, shown in Fig. 4-5 each have two tabs that are connected to anchor points on the tread using an axially stiff string, as the peeling coupler. The suction modules are made of two layers of silicone polymer and a resin base, to meet the corrosion resistance requirement (No. 4). The stiff backing layer (blue) of the suction modules is 2.5mm thick and made of Dragonskin 20 (SmoothOn, USA) silicone polymer and the soft ccntact layer (gray) is 2.5mm thick and made of Ecoflex 00-10 (SmoothOn, USA) silicone polymer.

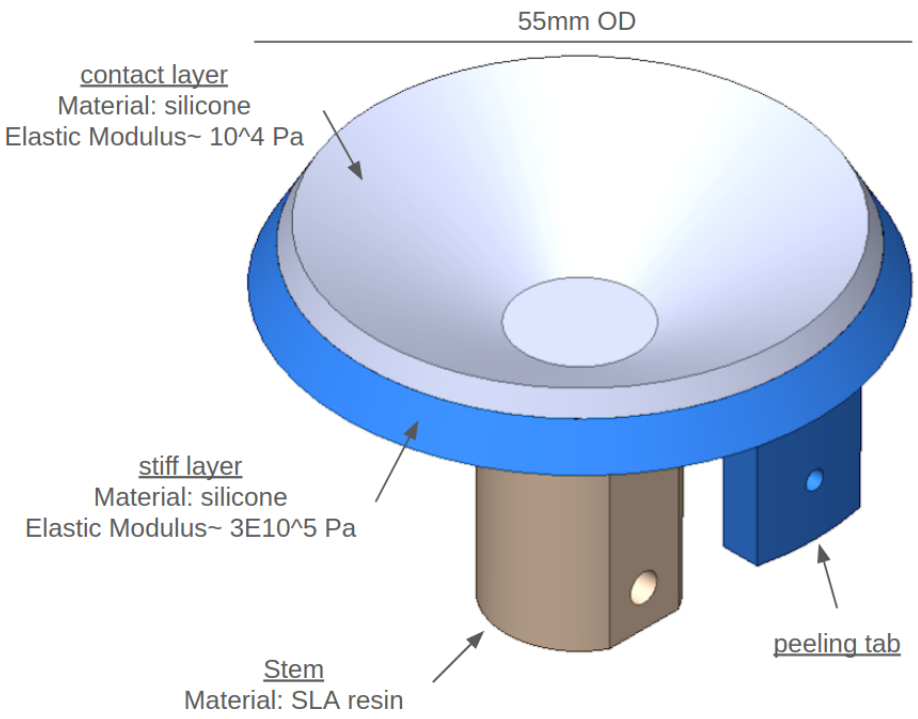

Figure 4-5: CAD model of bio-inspired suction module, with the strings not shown.

Peeling Mechanism

To meet functional requirement No. 1, each suction module traverses with the tread and elastically deforms and peels back when it gets to the curved portion of the tread in order to attach or detach to the substrate. Figure 4-6 shows a side view of the peeling mechanism. The suction module was designed to withstand the peeling force without material failure and the length of the suction modules were chosen to peel back by the appropriate amount as to cause the suction modules to peel back in order to attach and detach effectively.

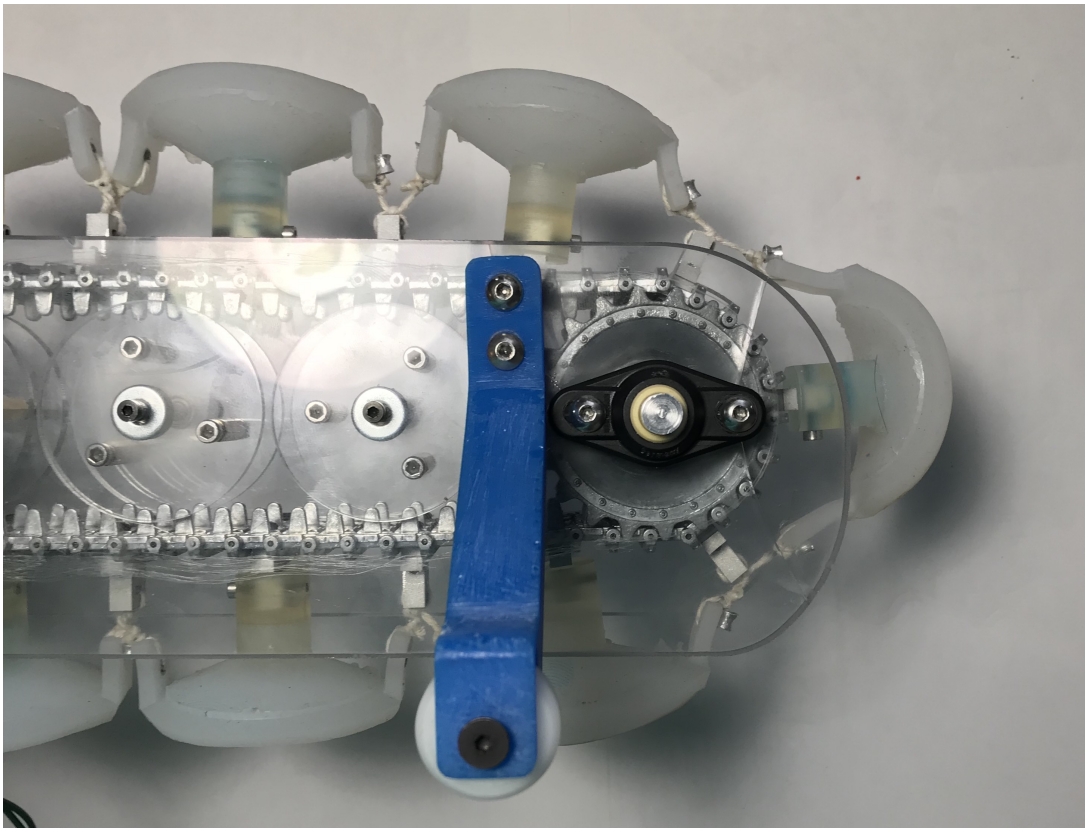

Figure 4-6: Picture of prototype, highlighting the attachment and locomotion mechanism.

4.2.4 Electronics

The electronics on the robot, shown in Fig. 4-7 consist of an arduino microcontroller board connected to a DRV8871 motor controller which controls a 9-24 Volt DC gearhead motor. A toggle switch controls the main power to the motor. The arduino microcontroller board allows for programming the motor controller to run a specific set of commands for performing tests on the prototype. The arduino and motor controller are housed inside a commercially available IP65 housing.

4.3 Fabrication

The prototype was fabricated and assembled in-house at MIT. The frame plates were machined using an Omax Waterjet. The training wheel structure was 3D printed on an FDM printer and the training wheels were turned on a prototrak lathe. The

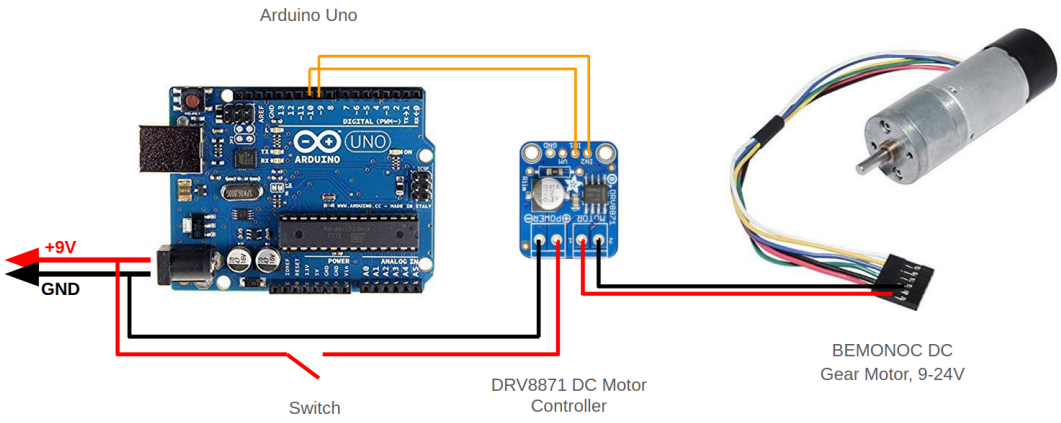

Figure 4-7: Diagram of the electronics of the prototype.

power transmission system shafts were Computer Numerical Control (CNC) machined using a prototrak lathe. The dual sprockets and tread links were purchased and post-machined on a prototrak mill to be retrofitted to the geometry of the prototype. The idler rollers were fabricated using a Universal laser cutter. Lastly, the suction modules were casted using silicone polymer on custom-designed molds. The details of the casting process and suction-module design are outlined below.

Suction Module

Each of the ten suction modules consists of a 3D printed resin stem that is overmolded with dual-material silicone polymer. The stems were 3D printed on a FormLabs 2 SLA printer using Clear V4 Form Labs resin. The molds were 3D printed on a Form 2 SLA printer. Figure 4-8 shows a CAD model of a mold used to make a single suction module. The spacers to set the spacing between the top and bottom molds, which controls the thickness of the silicone layers are not shown. The spacers were laser cut out of acrylic sheet.

Suction Module Molding Procedure

The molding procedure that was followed for each suction module is as follows:

1. Clean and wipe molds and stem with mineral spirits and let dry

2. Place stem into bottom base mold

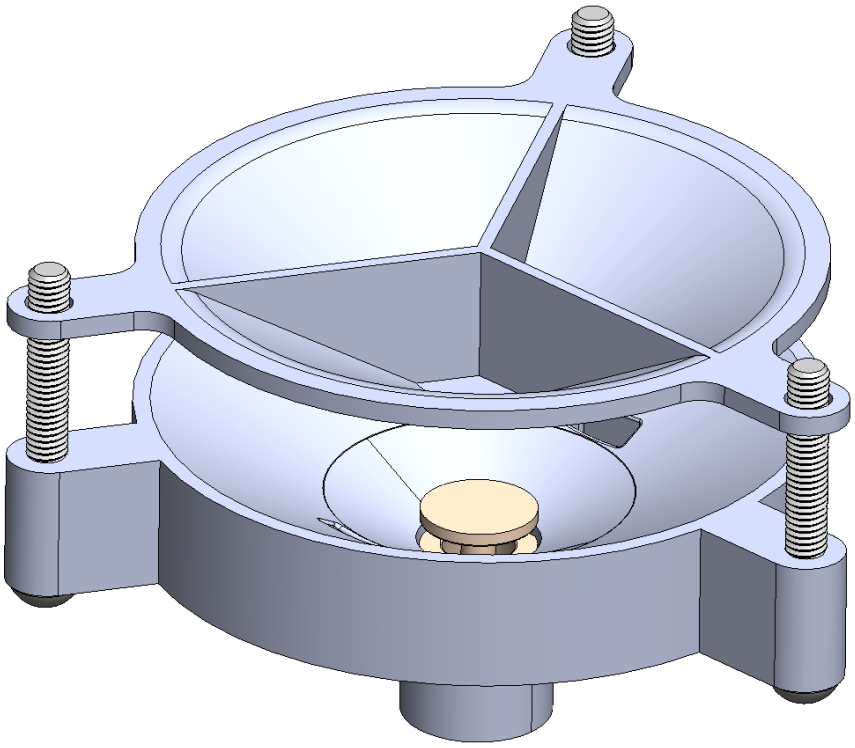

Figure 4-8: CAD model of suction module molds. Not shown: spacers to offset top and bottom molds.

3. Spray all inner surfaces of molds with mold-release (SmoothOn, USA)
4. Mix polymer for stiff backing layer, by hand in a glass beaker
5. Degas polymer in a vacuum chamber for approximately 10 minutes
6. Pour polymer into bottom mold assembly and degas for approximately 5 minutes
7. place a spacer on top of the bottom mold assembly and place the top mold over the bolts and secure with wing nuts
8. Let the assembly cure for the recommended cure time
9. Remove top mold and clean and wipe with mineral spirits and let dry
10. Spray top mold with mold release
11. Repeat steps 4-8 with the polymer for the soft contact layer

12. After curing, remove suction-module from molds and use a hole puncher to punch a hole in each tab of the suction module

4.4 Testing & Validation

In order to assess the functionality of the prototype, tests were performed in-air due to the fact that the robot was not designed to be fully submerged in water. Tests were performed on horizontal substrates, substrates with up to 30 degree incline and decline, and on horizontal substrates with obstacles in the way. The prototype performed as expected on horizontal substrates without obstacles in the way, maintaining attachment throughout a 6 foot straight line of locomotion. Figure 4-9 shows an example of a pull test done on the prototype showing that it maintained attachment 5 seconds after a straight line test on a horizontal substrate.

In tests with obstacles in the way, the prototype was able to successfully drive over the obstacles that were less than 5 cm in height. After driving over the obstacles and travelling a distance equivalent to one robot length, the robot was able to successfully attach under it's own weight and maintain attachment to the substrate. Figure 4-10 shows an example of the prototype driving over an obstacle.

The prototype consumed a total power of 10 Watts on horizontal surfaces and 25 Watts on surfaces inclined at 30 degrees. These preliminary tests prove the functionality of attachment and locomotion using continuous peeling of passive suction cups on a tread.

4.5 Future Work

The goal of the prototype was to test and validate the concept of continuous peeling of passive suction cups on a tread, as a means of attachment and locomotion, and initial tests validated the concept. We admit however, that several improvements must be implemented and several other tests must be performed in order for the device to

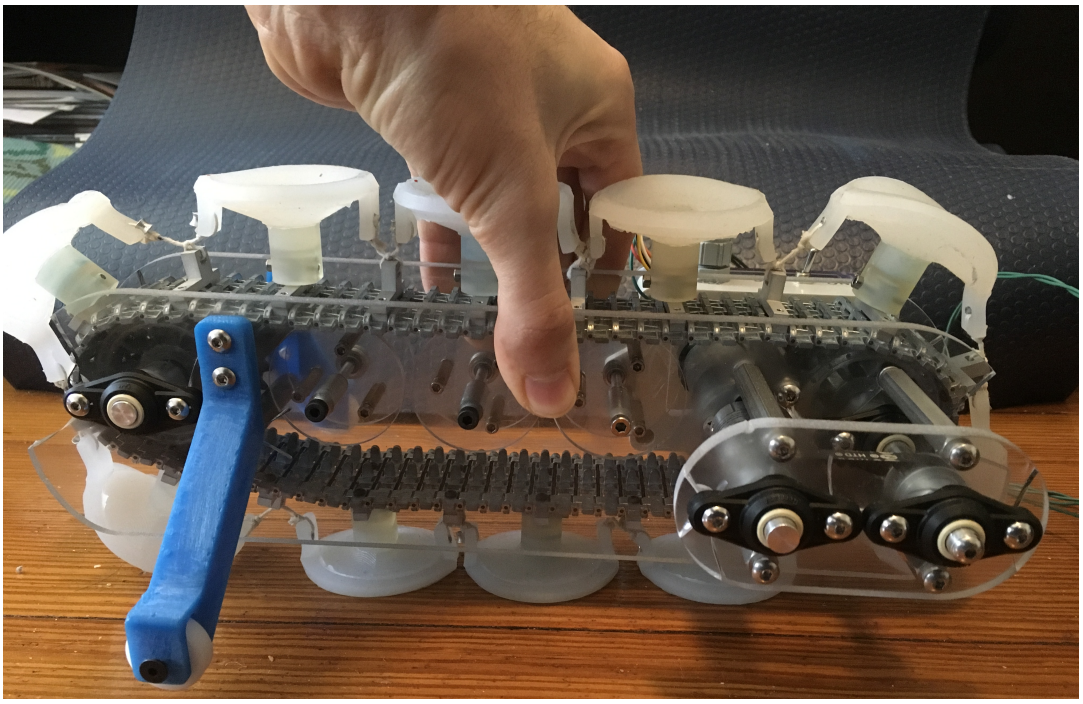

Figure 4-9: Image showing prototype maintaining attachment after a 6 foot straight line of locomotion.

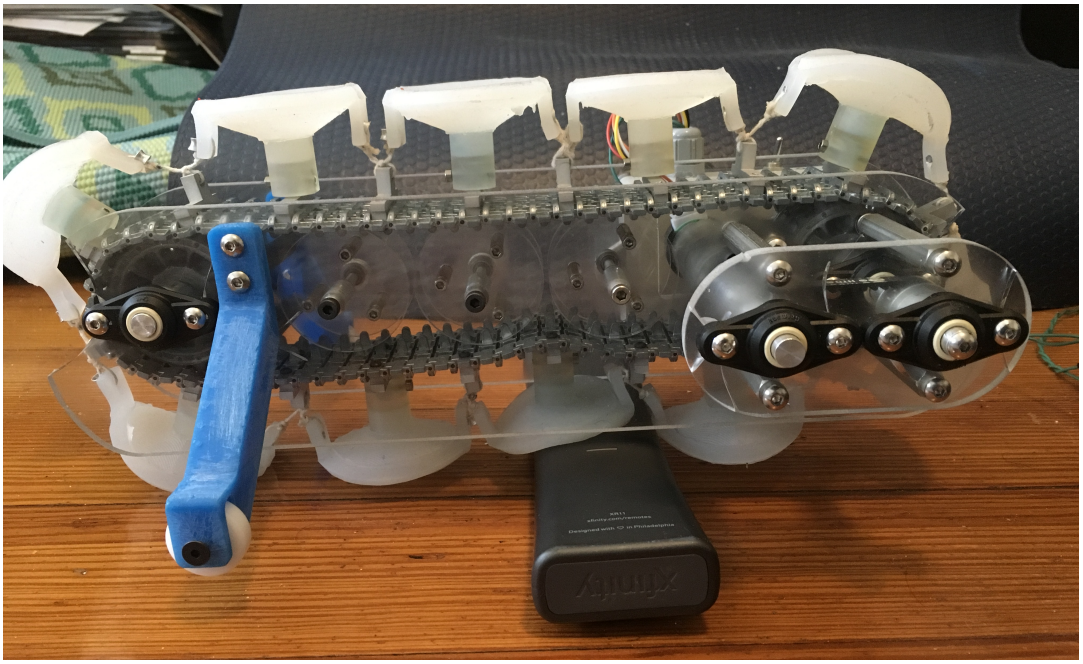

Figure 4-10: Prototype driving over an obstacle.

become robust enough for use in a real application. The major design improvements and future tests that we identify as the critical next steps are outlined below.

Design Improvements

The three critical design improvements that we believe need to be implemented in order to properly test a future prototype are:

- Waterproofing drive system and placing electronics on a bench
- Implementing a hydrodynamic shell
- improving peeling mechanism, reducing number of parts, reducing stress concentrations on suction cups

After the recommended improvements have been made to the design, a second, dual-track (two treads) prototype must be fabricated and tested. The two treads will stabilize the prototype and eliminate the need for training wheels and allow for the prototype to be tested more effectively in flow conditions.

Future Tests

In order to assess the feasibility of this mechanism in any real application, especially UVHC a critical next step is to perform tests in a tow tank, under flow conditions. The critical tests that will determine the feasibility of this device are:

- Task repeatability
- Maneuverability, ease of turning
- Detachment time in flow conditions
- Resistance to detachment forces
- Drag coefficient measurements

Under similar dynamic conditions, these tests can give more meaningful results than under static in-air conditions. The tests to measure preliminary drag coefficients should be performed in order to determine whether the attachment system can withstand the drag forces present in the application.

Chapter 5

Conclusion

The work presented in this thesis contributes to a more fundamental understanding of close-proximity suction-based attachment. This knowledge could facilitate the design and implementation of suction-based attachment mechanisms any application that can utilize close-proximity suction.

A thorough literature review of existing hull cleaning robots demonstrated that a new system design of an attachment and locomotion system was needed to make UVHC feasible for both ferrous and non-ferrous hulls. Since all of the existing solutions have come short of realizing UVHC, a new solution, inspired by nature was presented in this thesis and a proof-of-concept prototype was demonstrated. The passive bio-inspired suction cups were chosen as the attachment mechanism because of their ability to remain attached for long durations underwater with minimal input energy. Additionally, their compliance, cost and weight make them desirable in any application where crawling is required.

The new mechanism of continuous peeling of passive suction cups on a tread can be used on crawling and low-energy applications, as the main attachment system. A secondary active attachment system would supplement this one. The application of UVHC is one of many examples where this concept could be applied, however there are numerous other applications that could utilize this concept. This concept can be used for in-air attachment by spraying a more viscous fluid such as water on the suction cups before attachment, in order to improve detachment time. Moreover, a

suction cup cleaning mechanism can be implemented in order to clean the suction cups of any debris before spraying them with water for attachment. These are just some of the potential applications of this concept.

Finally, we present a sketch for new concept of an UVHC robot system design, utilizing the attachment and locomotion mechanism presented in this thesis. The concept, shown in Fig 5-1 resembles Raytheon's hull crawler, but relies on passive suction attachment with a back-up active suction attachment system for resisting the detachment forces.

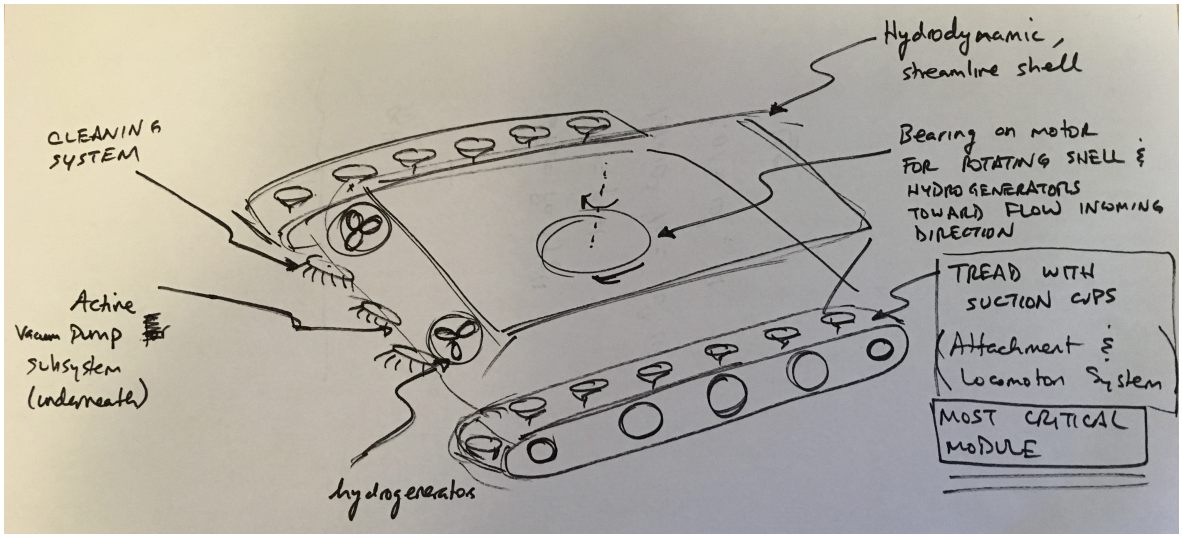

Figure 5-1: Attachment and Locomotion concept of continuous peeling of suction cups on a tread.

5.1 The Future of Vessel Hull Cleaning

The problems presented by marine bio growth may always exist to some degree or may disappear with the invention of new non-toxic and long-lasting coatings but until then we must use engineering solutions to combat it. Current vessel hull cleaning solutions such as dry-docking and in-port cleaning work and will continue to work, but we can do better. By pushing the boundaries of engineering, we can design a robust system that can increase the frequency of vessel hull cleanings and help fight the financial, health and environmental problems that bio-fouled vessels present.

The global economy will continue to become increasingly more global as populations grow and demand increases, and more vessels will continue to transport goods and people across the globe. This means that the problems will persist unless we find solutions to mitigate them. This work attempts to contribute a small fraction of knowledge towards finding a better solution to a more frequent vessel hull cleaning regimen.

Appendix A

First Order Calculation of Drag Force on a Hull Crawler

To calculate the drag force, given by Equation A.1, on a hull crawler to first order we assume a stationary hull crawler fully submerged underwater and attached to a moving, un-fouled merchant vessel, with the force balance on the hull crawler shown below.

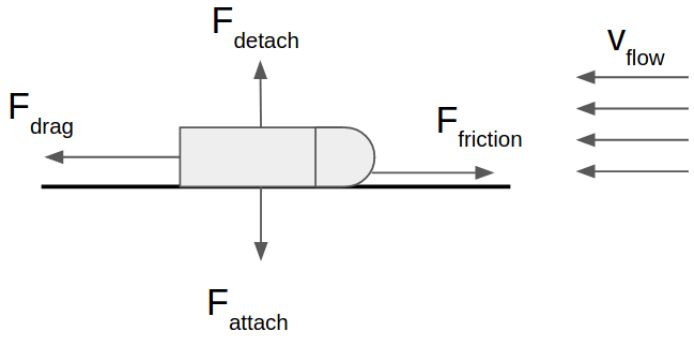

Figure A-1: Schematic showing the forces acting on a hull crawler.

$$F_{drag} = C_d \frac{1}{2} \rho v_{flow}^2 A_{ref} \tag{A.1}$$

Assumptions:

Merchant vessel maximum speed: 25 knots [7, 34]

Hull crawler cross-sectional area: $1m$ x $0.25m$

Coefficient of Drag: 1

Using these assumptions, the drag force is computed to be 21 kN. Figure A-2 below, shows this drag force as a function of the coefficient of drag at three different flow velocities. The coefficient of drag of a streamlined body and a half sphere are labeled, for reference.

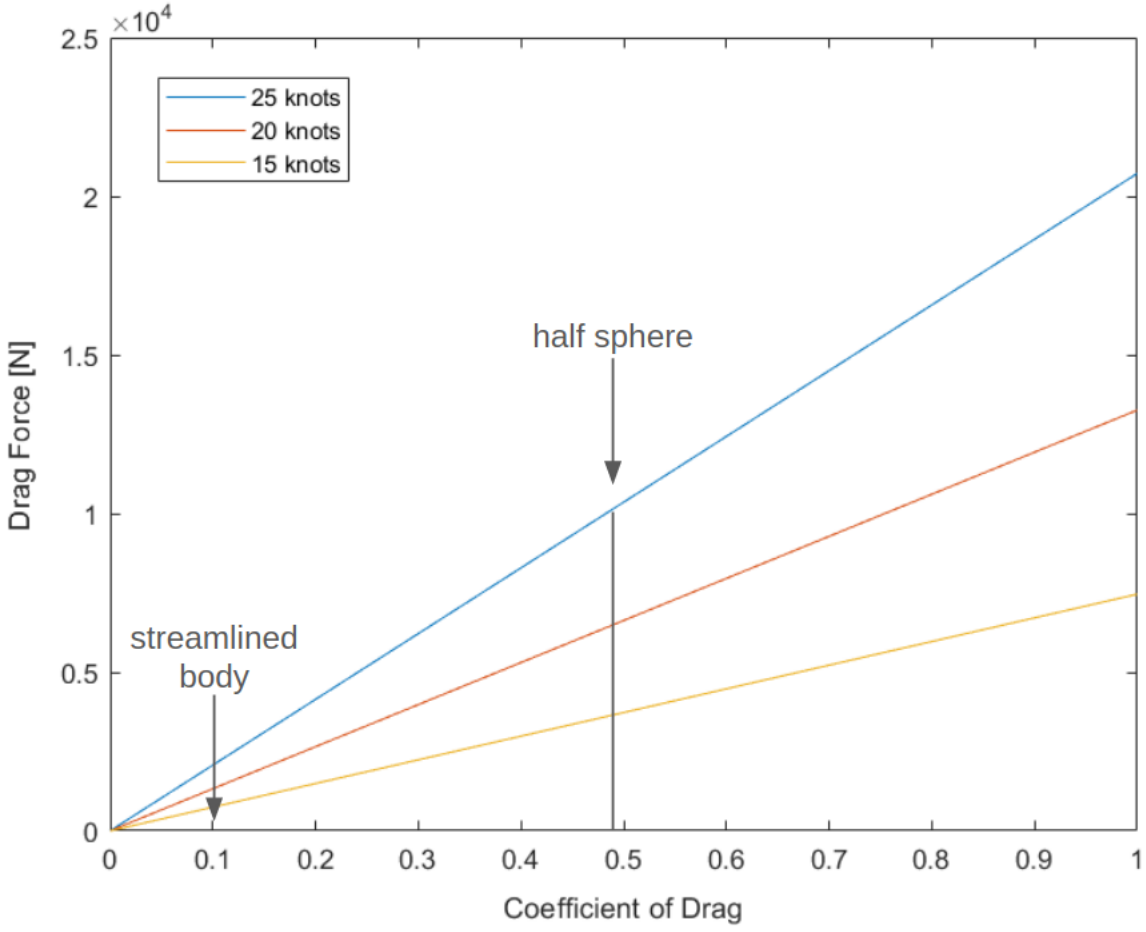

Figure A-2: Calculation of drag force acting on a hull crawler as a function of the coefficient of drag, at three flow velocities.

Appendix B

Watt & Sea POD 600 Hydrogenerator Information

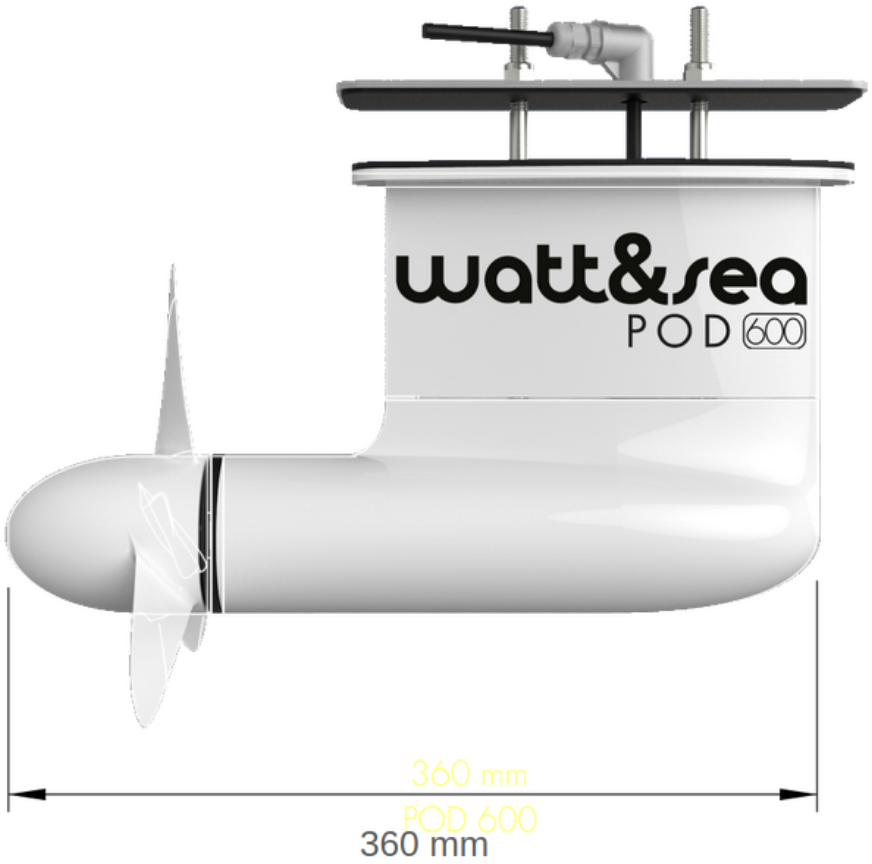

Figure B-1: Watt & Sea POD 600 hydrogenerator.

Figure B-2 the shows power generation data for the Watt & Sea POD 600 hydrogenerator.

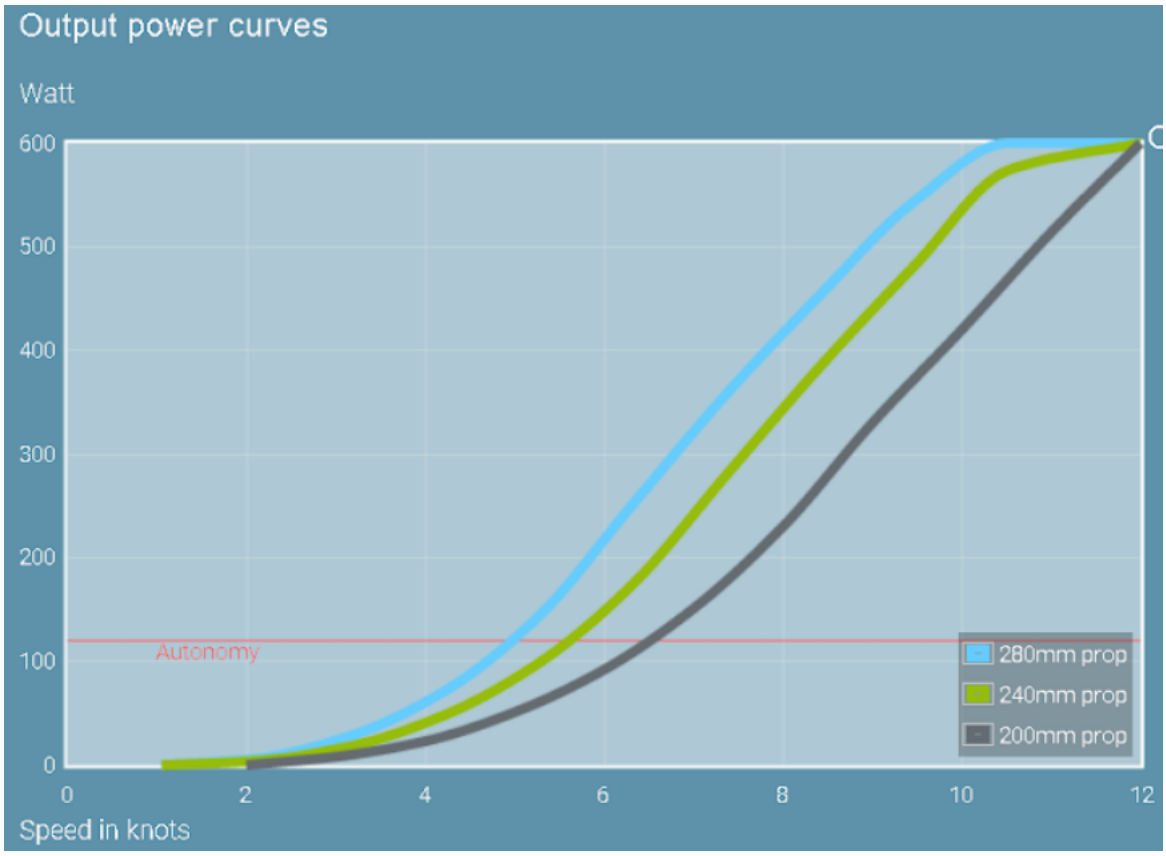

Figure B-2: Watt & Sea POD 600 hydrogenerator power generation plot.

Bibliography

[1] Teodor Akinfiev, Alexander Janushevskis, and Egons Lavendelis. "A brief survey of ship hull cleaning devices". In: *Transport and Engineering* 24 (2007), pp. 133–146.

[2] Houssam Albitar, Anani Ananiev, and Ivan Kalaykov. "In-water surface cleaning robot: concept, locomotion and stability". In: *International Journal of Mechatronics and Automation* 4.2 (2014), p. 104. ISSN: 2045-1059. DOI: 10.1504/IJMA.2014.062338. URL: http://www.scopus.com/inward/record.url?eid=2-s2.0-84904859302&partnerID=tZOtx3y1.

[3] Agamemnon Apostolidis, John Kokarakis, and Andreas Merikas. "Modeling the dry-docking cost - The case of tankers". In: *Transactions - Society of Naval Architects and Marine Engineers* 120.3 (2013), pp. 447–456. ISSN: 00811661.

[4] BCC. *Water Transportation Market Global Briefing 2019*. Tech. rep. June. 2019.

[5] M. Beckert, B. E. Flammang, and J. H. Nadler. "Remora fish suction pad attachment is enhanced by spinule friction". In: *Journal of Experimental Biology* 218.22 (2015), pp. 3551–3558. ISSN: 0022-0949. DOI: 10.1242/jeb.123893.

[6] Gregory D. Bixler and Bharat Bhushan. "Review article: Biofouling: Lessons from nature". In: *Philosophical Transactions of the Royal Society A: Mathematical, Physical and Engineering Sciences* 370.1967 (2012), pp. 2381–2417. ISSN: 1364503X. DOI: 10.1098/rsta.2011.0502.

[7] Moritz Bollmann et al. "Maritime highways of global trade". In: *World ocean review: Living with the oceansr* (), pp. 164–175.

[8] Eric Brown et al. "Universal Robotic Gripper based on the Jamming of Granular Material". In: (2010). DOI: 10.1073/pnas.1003250107. URL: http://arxiv.org/abs/1009.4444%0Ahttp://dx.doi.org/10.1073/pnas.1003250107.

[9] University of California. *West Coast Ballast Outreach*. URL: http://ballast-outreach-ucsgep.ucdavis.edu/Non-Ballast_Vessel_Vectors/Hull_Fouling_Research_and_Reports/%0A.

[10] Y. Chen et al. "Underwater attachment using hairs: the functioning of spatula and sucker setae from male diving beetles". In: *Journal of The Royal Society Interface* 11.97 (2014), pp. 20140273–20140273. ISSN: 1742-5689. DOI: 10.1098/rsif.2014.0273. URL: http://rsif.royalsocietypublishing.org/cgi/doi/10.1098/rsif.2014.0273.

[11] A. Curran et al. “Analyzing the current market of hull cleaning robots”. In: (2016).

[12] P. Ditsche, D. K. Wainwright, and A. P. Summers. “Attachment to challenging substrates - fouling, roughness and limits of adhesion in the northern clingfish (Gobiesox maeandricus)”. In: *Journal of Experimental Biology* 217.14 (2014), pp. 2548–2554. ISSN: 0022-0949. DOI: 10.1242/jeb.100149.

[13] Petra Ditsche and Adam Summers. “ Learning from Northern clingfish (Gobiesox maeandricus): bioinspired suction cups attach to rough surfaces ”. In: *Philosophical Transactions of the Royal Society B: Biological Sciences* 374.1784 (2019), p. 20190204. ISSN: 0962-8436. DOI: 10.1098/rstb.2019.0204.

[14] Petra Ditsche and Adam P. Summers. “Aquatic versus terrestrial attachment: Water makes a difference”. In: *Beilstein Journal of Nanotechnology* 5.1 (2014), pp. 2424–2439. ISSN: 21904286. DOI: 10.3762/bjnano.5.252.

[15] Petra Ditsche et al. “From smooth to rough, from water to air: The intertidal habitat of northern clingfish (Gobiesox maeandricus)”. In: *Science of Nature* 104.3-4 (2017). ISSN: 14321904. DOI: 10.1007/s00114-017-1454-8.

[16] Randy H Ewoldt et al. “Controllable adhesion using field-activated fluids Controllable adhesion using field-activated fluids”. In: 073104.2011 (2014), pp. 1–15. DOI: 10.1063/1.3608277.

[17] *Fleet Cleaner*. URL: www.fleetcleaner.com/.

[18] M. Follador, F. Tramacere, and B. Mazzolai. “Dielectric elastomer actuators for octopus inspired suction cups”. In: *Bioinspiration and Biomimetics* 9.4 (2014). ISSN: 17483190. DOI: 10.1088/1748-3182/9/4/046002.

[19] *HullWiper*. URL: www.hullwiper.co.

[20] *HullWiper partners with GAC to introduce eco-friendly hull cleaning solution in Qatar*. 2020. URL: www.hullwiper.co/news/hullwiper-partners-with-gac-to-introduce-eco-friendly--hull-cleaning-solution-in-qatar/.

[21] *International Chamber of Shipping*. URL: https://www.ics-shipping.org/shipping-facts/key-facts.

[22] *Invert Robotics*. URL: www.invertrobotics.com/robotic-crawler.

[23] *K&J Magnetics*. URL: www.kjmagnetics.com.

[24] Chad C. Kessens and Jaydev P. Desai. “A Self-Sealing Suction Cup Array for Grasping”. In: *Journal of Mechanisms and Robotics* 3.4 (2011), p. 045001. ISSN: 19424302. DOI: 10.1115/1.4004893.

[25] Jennifer Lauv et al. *Hull Crawler Whitepaper*. Tech. rep. MIT, 2017.

[26] *Marine fouling and its prevention*. Tech. rep. 580. Woods Hole Oceanographic Institution, 1952, pp. 1–388. DOI: 10.1575/1912/191.

[27] Tohru Miyake, Hidenori Ishihara, and Motoi Yoshimura. "Basic studies on wet adhesion system for wall climbing robots". In: *IEEE International Conference on Intelligent Robots and Systems* (2007), pp. 1920–1925. DOI: 10.1109/IROS.2007.4399417.

[28] *National Maritime Historical Society*. URL: https://seahistory.org/sea-history-for-kids/worms-and-barnacles-and-algae-oh-my/.

[29] B. N.J. Persson. "On the theory of rubber friction". In: *Surface Science* 401.3 (1998), pp. 445–454. ISSN: 00396028. DOI: 10.1016/S0039-6028(98)00051-X.

[30] B. N.J. Persson et al. "On the nature of surface roughness with application to contact mechanics, sealing, rubber friction and adhesion". In: *Journal of Physics Condensed Matter* 17.1 (2005). ISSN: 09538984. DOI: 10.1088/0953-8984/17/1/R01.

[31] *PIAB*. URL: www.piab.com.

[32] D H I Prb. "DHI Vessel Hull Data Sheets Data Sheets for Different Vessels". In: (2017).

[33] Alexander Railkin, Tatiana Ganf, and Oleg Manylov. "Biofouling as a Process". In: *Marine Biofouling* 1 (2003), pp. 25–39. DOI: 10.1201/9780203503232.ch2.

[34] Shipping Safety Record. "LNG Information Paper No . 3 LNG Ships". In: *Training* 3 (2009), pp. 1–7.

[35] A. D. Roberts. "A Guide to Estimating the Friction of Rubber". In: *Rubber Chemistry and Technology* 65.3 (1992), pp. 673–686. DOI: 10.5254/1.3538633.

[36] James H. Rooney III et al. *Hull Robot with Rotatable Turret*. 2009.

[37] Bill Ross, John Bares, and Chris Fromme. "A Semi-Autonomous Robot for Stripping Paint from Large Vessels". In: *The International Journal of Robotics Research* 22.7-8 (2003), pp. 617–626. ISSN: 0278-3649. DOI: 10.1177/02783649030227010. URL: http://journals.sagepub.com/doi/10.1177/02783649030227010.

[38] Maria Salta et al. "Designing biomimetic antifouling surfaces". In: *Philosophical Transactions of the Royal Society A: Mathematical, Physical and Engineering Sciences* 368.1929 (2010), pp. 4729–4754. ISSN: 1364503X. DOI: 10.1098/rsta.2010.0195.

[39] M. P. Schultz et al. "Economic impact of biofouling on a naval surface ship". In: *Biofouling* 27.1 (2011), pp. 87–98. ISSN: 08927014. DOI: 10.1080/08927014.2010.542809.

[40] Michael P. Schultz. "Effects of coating roughness and biofouling on ship resistance and powering". In: *Biofouling* 23.5 (2007), pp. 331–341. ISSN: 08927014. DOI: 10.1080/08927010701461974.

[41] Kaige Shi and Xin Li. "Vacuum suction unit based on the zero pressure difference method". In: *Physics of Fluids* 32.1 (2020). ISSN: 10897666. DOI: 10.1063/1.5129958. URL: https://doi.org/10.1063/1.5129958.

[42] D. Souto et al. "Lappa: A new type of robot for underwater non-magnetic and complex hull cleaning". In: *Proceedings - IEEE International Conference on Robotics and Automation* (2013), pp. 3409–3414. ISSN: 10504729. DOI: 10.1109/ICRA.2013.6631053.

[43] D. Sperling and M. A. Deluchi. *Transportation energy futures*. 1989, pp. 375–424. ISBN: 1800553684. DOI: 10.1146/annurev.energy.14.1.375.

[44] J. Stefan. "Versuche zur scheinbaren Adhesion". In: *Annalen der Physik und Chemie* 154 (1875), pp. 316–318.

[45] *Teledyne Marine*. URL: www.teledynemarine.com/vlbc.

[46] Francesca Tramacere et al. "Structure and mechanical properties of Octopus vulgaris suckers". In: *Journal of the Royal Society Interface* 11.91 (2014). ISSN: 17425662. DOI: 10.1098/rsif.2013.0816.

[47] Melissa Tribou and Geoffrey Swain. "The use of proactive in-water grooming to improve the performance of ship hull antifouling coatings". In: *Biofouling* 26.1 (2010), pp. 47–56. ISSN: 08927014. DOI: 10.1080/08927010903290973.

[48] UNCTAD. *Reveiw of Maritime Transport*. 2018, p. 29. ISBN: 9789211129281. DOI: 10.18356/a9b345e7-en. URL: https://unctad.org/en/PublicationsLibrary/rmt2018_en.pdf.

[49] United States Environmental Protection Agency (EPA). "Underwater ship husbandry discharges". In: *United States Environmental Protection Agency* November (2011). DOI: 10.4043/2401-MS.

[50] Yueping Wang et al. "A biorobotic adhesive disc for underwater hitchhiking inspired by the remora suckerfish". In: *Science Robotics* 2.10 (2017), eaan8072. ISSN: 2470-9476. DOI: 10.1126/scirobotics.aan8072. URL: http://robotics.sciencemag.org/lookup/doi/10.1126/scirobotics.aan8072.

[51] Ying Xu et al. "Mussel-Inspired Polyesters with Aliphatic Pendant Groups Demonstrate the Importance of Hydrophobicity in Underwater Adhesion". In: *Advanced Materials Interfaces* 4.22 (2017), pp. 1–6. ISSN: 21967350. DOI: 10.1002/admi.201700506.

[52] Fut Kuo Yang and Boxin Zhao. "Adhesion Properties of Self-Polymerized Dopamine Thin Film". In: *The Open Surface Science Journal* 3.1 (2014), pp. 115–122. ISSN: 18765319. DOI: 10.2174/1876531901103010115.